Microchim Acta (2017) 184:343–368
DOI 10.1007/s00604-016-2043-9

REVIEW ARTICLE

Carbon dots doped with heteroatoms for fluorescent bioimaging: a review

Jin Zhou[1] · Hui Zhou[1] · Jinbao Tang[1] · Shue Deng[1] · Fang Yan[1] · Wenjing Li[1] · Meihua Qu[1]

Received: 29 September 2016 / Accepted: 2 December 2016 / Published online: 19 December 2016

Abstract Carbon dots (CDs) possess superior fluorescent properties in that they do not blink, are biocompatible, chemically inert, have small size and well tunable photoluminescence (PL), can be easily functionalized with biomolecules, and can be multi-photon excited to give up-converted PL. This review (with 141 refs.) summarizes recent progress in the field of imaging using carbon dots doped with heteroatoms (X-CDs). Following an introduction, we discuss top-down and bottom-up strategies for synthesis and methods for surface modification. We also compare the differences in synthesis for undoped CDs and X-CDs. Specifically, CDs doped with heteroelemets nitrogen, phosphorus, sulfur, selenium, boron and silicium are treated. We then discuss method for determination of the properties (particle size, ZP), how doping affects fluorescence (spectra, quantum yields, decay times), and how dopants affect upconversion (UC, anti-Stokes luminescence). We finally review the progress made in fluorescent imaging of cells tissue, and other biomatter. This review also gives new hints on how to use synthetic methods for tuning the structure of X-CDs, how doping affects properties, and how to achieve new bioimaging applications.

Keywords Carbon-based materials · Photoluminescence · Quantum yield · Upconversion · Surface functionalization · Decay times · Tissue imaging · Cellular imaging · Near infrared light

✉ Jin Zhou
zhoujin@wfmc.edu.cn

[1] Key Lab of Applied Pharmacology in Universities of Shandong, College of Pharmacy, Institute of Nanomedicine Research, Weifang Medical University, Weifang 261053, China

Introduction

Carbon-based materials have attracted increasing attention due to their outstanding merits such as low toxicity, biocompatibility and chemical stability [1]. The advantageous properties of carbon-based materials make them promising candidates for numerous exciting applications [2–5]. Carbon dots (CDs) is a representative member among these materials. CDs mainly consisting of graphene quantum dots (GQDs), carbon nanodots (CNDs) and polymer dots (PDs) are a new kind of carbon nanomaterials with sizes usually below 10 nm, which have attracted tremendous research interest since their discovery during the purification of single-walled carbon nanotubes in 2004 [6]. CDs are categorized by the inner structure of the carbon in the small dots [7]. GQDs usually refer to nanographene fragments whose diameters are less than 10 nm with a single or a few layers. GQDs, in fact, are not graphenes because they contain substantial fractions of oxygen and hydrogen, and also display fluorescence which pure graphene does not display at all. CNDs are defined comprehensively as spherical carbon materials in the nanoscale no matter whether they are made up of sp^2 carbon or amorphous aggregations. PDs represent the CDs those are formed from polymers during the cross-linking and dehydration. For the sake of convenience, the above three kinds of nanosized carbon materials are comprehensively termed as CDs. Due to their fascinating properties, CDs have drawn much attention in many fields [8]. For example, CDs have gradually become a rising star as drug-delivery vehicles because of their small size while allowing real-time monitoring of releasing kinetics [9]. Furthermore, their ideal electro- or photo- catalytic feature is applied in environmental protection and energy conservation [10,

11]. CDs have also been used as biosensor carriers for their flexibility in surface modification and solubility in water [12–14].

Among the excellent features, fluorescent property of CDs is one of the most exciting for researchers in materials and biological science. Fluorescence spectroscopy has aroused much attention because of high sensitivity and spatiotemporal resolution [15–18]. Compared to semiconductor quantum dots (QDs), CDs emerge as superior fluorophores in terms of low toxicity, good biocompatibility, excellent photostability, exceptional multi-photon excitation photon excitation property, and ease to be functionalized with biomolecules, which shows broad application prospect in the area of biomedicine [19]. Particularly, in application for fluorescent bioimaging, dozens of reports have indicated that CDs can be taken up into living cells via endocytosis and remain fluorescent in various cellular locations, demonstrating the bioimaging capability of CDs [7, 20, 21]. As a potential fluorescent probe for long- or real-time bioimaging, which is a significant way to disclose the cell functions dynamically, it is necessary to make further efforts to improve the fluorescent properties of CDs. It is found that doping CDs with heteroatoms (X-CDs) may modulate the properties of CDs and expand their applications in fluorescent bioimaging.

Since the synthesis, properties, underlying mechanisms and promising applications of CDs have already been systematically elaborated elsewhere [22–28], we will concentrate our horizons on X-CDs and their biological applications especially in fluorescent bioimaging. In this review, we describe the recent progress in the field of X-CDs, mainly focusing on the design strategies, doping methods, optical properties, fluorescent mechanism, and latest biological application in fluorescent imaging, which may be useful to readers who are interested in the continually growing research area.

Synthetic strategies

Generally, synthesis of X-CDs can be classified in to "top-down" and "bottom-up" strategies. The "top-down" strategy refers to synthesis of X-CDs through cleaving or breaking down of large-sized carbonaceous materials by chemical, electrochemical, or physical methods when heteroatoms have already been doped in the carbonaceous materials before the "top-down" process or are doped during the process. On the contrary, the "bottom-up" strategy is realized via pyrolysis or self-assembly of small organic molecules containing heteroatoms as the precursors to form relatively larger and more complicated system by the interactions between the precursors. Some typical strategies on synthetic methods, precursors, quantum yields, etc. are listed in Table 1.

Top-down strategy

Acidic oxidation

Strong acid such as concentrated sulfuric acid and/or concentrated nitric acid treatment have been widely used to prepare X-CDs via exfoliation and cleaving from graphene oxide (GO) [29], carbon nanotubes (CNTs) [30], carbon fibers [31], soot [32], activated carbon and so on [33], which are feasible for large-scale solution-processable synthesis from readily available low-cost carbon materials by means of simple operation (such as Fig. 1). Such methods not only unavoidably introduce negatively charged oxygenated groups onto the resultant carbon nanodots, making them hydrophilic and defective in graphitic structure, but also adjust the size and ectochemisty of CDs, tailoring the efficient band gap efficiently to make them emit different fluorescence (blue, green, yellow, red and near-IR). The heteroatom such as nitrogen was doped into the CDs from the oxidizing agent (e.g. HNO_3). It is another good choice to chemically oxidize heteroatom-doped carbon materials to obtain X-CDs with much more content of heteroatoms. For example, Qian et al. synthesized a kind of nanosized nitrogen-doped graphene oxide by chemical oxidation of mixed concentrated acids (H_2SO_4: HNO_3) [34]. Phosphorous- and nitrogen-codoped X-CDs were synthesized by HNO_3 oxidation of phosphorous-doped X-CDs [35]. However, there are still some disadvantages for acidic oxidation, such as harsh conditions and time-consuming process to eliminate excessive acid.

Hydrothermal or solvothermal synthesis

Hydrothermal synthesis refers to the chemical reaction occurred in water, being sealed in container under high temperature and pressure, which is a simple and green method. As is known, solvothermal synthesis expands the hydrothermal method, in which some organic solvents can also be used as the solvents [23]. To synthesize X-CDs, Hydrothermal synthesis typically uses thermally reduced or oxidized GO or CNTs as the precursors that possess defects as the cleavage sites on the carbon lattice. Under hydrothermal/sovothermal conditions, X-CDs with fluorescent property are finally produced by by the formation of zig-zag sits. Zhu et al. demonstrated the first solvothermal synthesis of X-CDs on a large scale with a quantum yield of 11.4% from GO sheets using DMF as solvent via one-step solvothermal route [36]. Hu et al. Obtained highly fluorescent nitrogen-doped X-CDs by hydrothermal treatment of GO in the presence of ammonia, then applied them for bioimaging of HeLa

Table 1 A brief summary of the properties of partial X-CDs prepared by various synthesis and modification methods

Methods	Details	Starting materials	PL color	QY (%)	Ref.
Top-down	Acidic oxidation	CNTs	Yellow	6	30
	Acidic oxidation	carbon fiber	Blue to yellow	–	31
	Acidic oxidation	activated carbon	Blue	12.6	33
	Acidic oxidation	graphitic carbon nitride	Blue	90.2	35
	Solvothermal treatment	GO	Green	11.4	36
	Hydrothermal treatment	GO	Blue	24.6	37
	Electrochemical method	Graphene film	Blue	–	39
	Electrochemical method	Graphite rod	Yellow	14	40
	Electrochemical method	3D grphene	Blue	10	41
	Electrochemical method	Graphite	Blue	10.6	43
	Laser ablation	Graphite	Blue to red	10	44
	Microwave irradiation	GO nanosheets	Greenish yellow	22.9	45
	Ultrasonication	GO	Blue (UC)	3.4	46
	Ultrasonication	Graphitic carbon nitride	Blue	–	47
Bottom-up	solvothermal synthesis	Citric acid, formamide	Blue to red	26.2	49
	solvothermal synthesis	Phenylenediamine	Blue to red	20.6	50
	Microwave method	Folic acid	Blue	18.9	51
	Microwave method	Phosphorus-rich phytic acid	Green	19.5	52
	Microwave method	Citric acid, thiourea	Green	31.6	53
Surface treatment	Multi-step	EDTA, spiropyran	Green to red	15	54
	Multi-step	Oxaliplatin, CDs	Red	21.0	55
	Multi-step	a photosensitizer, C-dots	Red	2	56
	Multi-step	Silica nanoparticles, CDs	Red	25	57
	One-step	GO, ammonia, hydrogen peroxide	Green	4.4	58
	One-step	Polyethylenimine, citric acid	Blue	42.5	59

cells, and showed bright fluorescence and excellent biocompatibility (Fig. 2) [37].

Electrochemical exfoliation

It is a facile, green and large-scale approach to synthesize X-CDs by electrochemical exfoliation, avoiding the use of excessively concentrated acid and complex purification and separation procedures. X-CDs in electrochemical exfoliation approach were first reported by Lu et al. [38]. During the process, they used high high-purity graphite rods and highly oriented pyrolytic graphite as anode and Pt wire as counter-electrode in the ionic liquid electrolyte of 1-butyl-3-methylimidazolium tetrafluoroborate $[BMI_m][BF_4]$ with water at different fractions, obtaining boron-, fluorine- and nitrogen-codoped X-CDs. The mechanism of the exfoliation was presented that OH• and O• radicals formed from anodic oxidation of water act as electrochemical "scissors" to release CDs (Fig. 3) [38]. The repeatability of the chemical composition and the surface passivation of the exfoliated X-CDs is restricted due to the change in the ratio of the ionic liquid to water in the electrolyte [26].

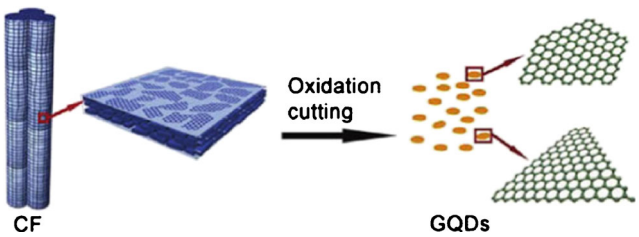

Fig. 1 Representation scheme of oxidation cutting of carbon fibre (CF) into CDs. Produced with permission from ref. [31]

Functional heteroatoms may be doped onto the resultant CDs depending on the electrolyte used. Li et al. pioneered making nitrogen-doped CDs in electrochemical method which applied a high potential of 3 V to drive the nitrogen-containing electrolyte ions into the graphene layers and oxidize the C-C bonds of the graphene sheets in one step [39]. Subsequently, via electrochemical oxidative cleavage, Zhang et al. synthesized nitrogen-doped C-dots with yellow fluorescence for use in stem cell labeling [40]. Ananthanarayanan et al. preprared the nitrogen-doped CDs by electrochemical cutting of the graphene 3D framework [41]. Similarly, the dopant of boron or sulfur was incorporated into CDs [42, 43].

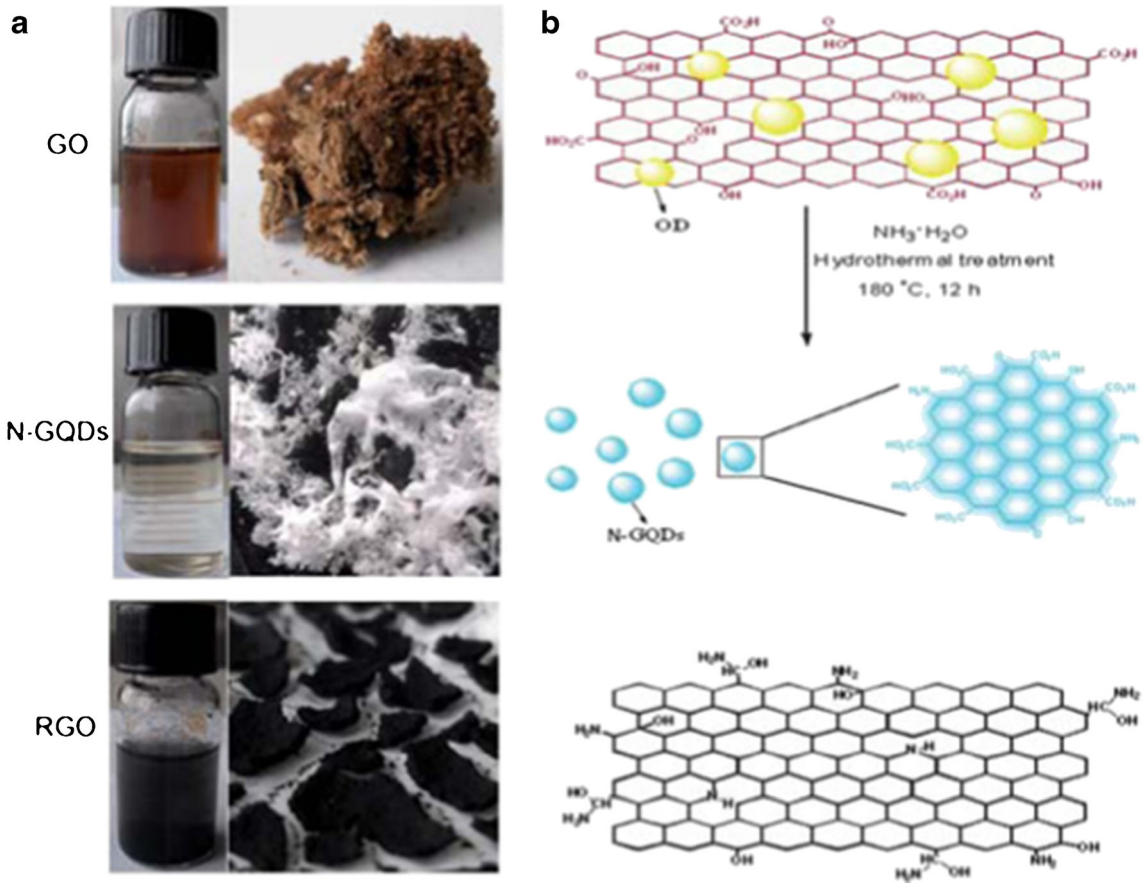

Fig. 2 **a** Typical pictures of water dispersions and solid samples of GO, N-GQDs (nitrogen-doped CDs) and RGO (chemically reduced GO). **b** Schematic illustration for the preparation of nitrogen-doped CDs by hydrothermal treatment of GO in the presence of ammonia. Produced with permission from ref. [37]

Physical routes

As high-energy technology, laser, microwave and ultrasonic shearing is capable of cutting large-sized carbonaceous materials into CDs, which thus dramatically shortens the synthesis time. Laser ablation is the method by laser irradiation of carbonneous precursors. Sun et al. first prepared nitrogen-doped CDs via high power laser irradiation and subsequent treatment of acid and passivation [44], while this means is limited by the need of sophisticated equipment. Microwave irradiation has the advantage of rapid and uniform heating of the reaction medium, improving the product quality effectively. As shown in Fig. 4, different fluorescent CDs are also prepared via cleaving and reduction processes of GO simultaneously using microwave treatment [45]. Ultrasound can lead to violent collapse of small vacuum bubbles, producing strong hydrodynamic shear forces to break down the layered carbon structures [46]. Tian et al. synthesized ultrathin fluorescent CDs with the thickness of 1.0 nm by ultrasonication-assisted liquid exfoliation of graphitic carbon nitride in water [47].

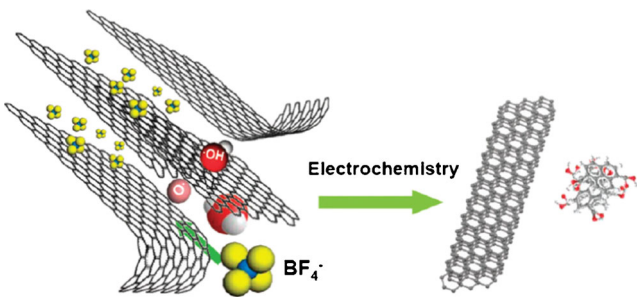

Fig. 3 Illustration of the exfoliation process showing the attack of the graphite edge planes by hydroxyl and oxygen radicals, which facilitate the intercalation of BF_4^- anion. The dissolution of hydroxylated carbon nanoparticles gives rise to the fluorescent carbon nanoparticles. Oxidative cleavage of the expanded graphite produces graphene nanoribbons. Produced with permission from ref. [38]

Bottom-up strategy

Compared with top-down strategy, the bottom-up strategy has obvious advantages in adjusting the composition by the careful selection of various organic precursors.

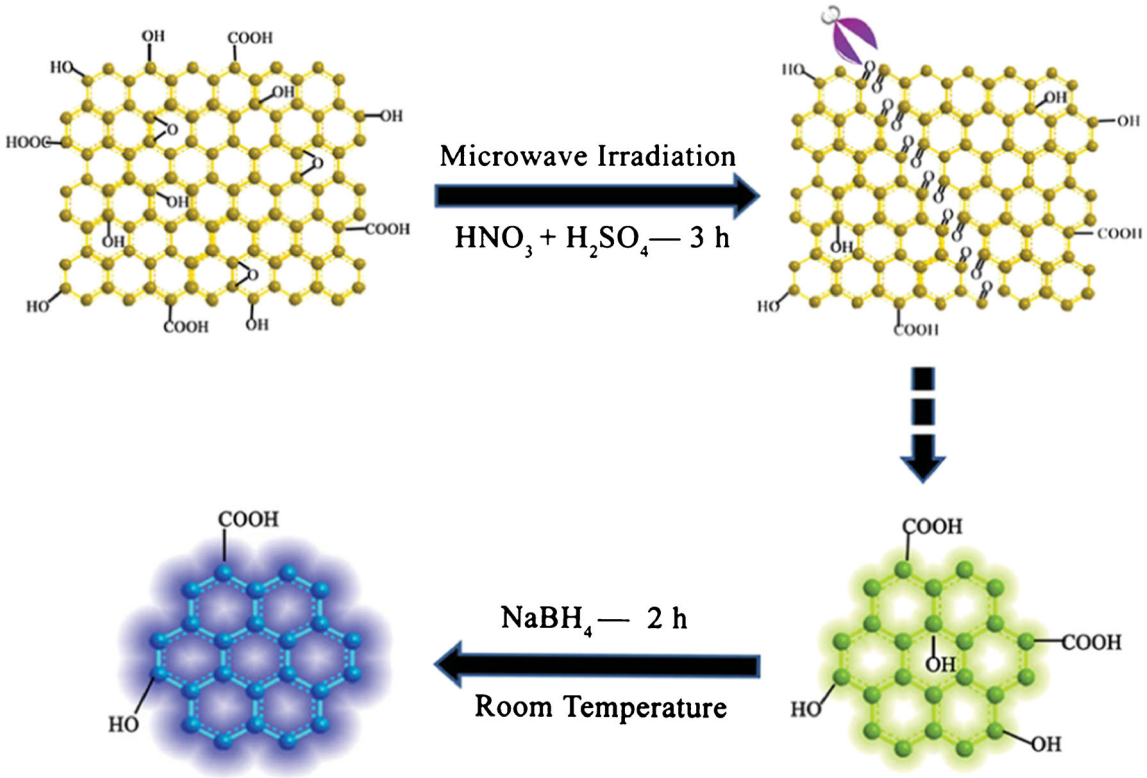

Fig. 4 Schematic representation of the preparation route for X-CDs. Produced with permission from ref. [45]

Hydrothermal or solvothermal synthesis

Synthesis of X-CDs by hydrothermal or solvothermal method has been widely reported. The precursors of small molecules in water or organic solvents occur reaction in a sealed container under high temperature and pressure [48]. The direct rise of temperature may come from the microwave heating or other heating method. A microwave assisted synthesis of fluorescent X-CDs from citric acid molecules as carbon source and formamide as the nitrogen source and solvent was explored by Pan et al. [49]. In brief, citric acid formamide solution was transferred into a Teflonlined autoclave and was heated in a microwave chemical reactor, then the reaction mixture was subjected to dialysis for removing the unreacted starting materials. By changing the reaction time and tempeture, X-CDs with different fluorescence can be obtained. Another typical example is the X-CDs with full-color emission synthesized by Jiang et al. [50]. Alterations of red, green and blue fluorescent emission of these X-CDs are presented to result to the difference in their particle size and nitrogen content (Fig. 5). Interestingly, UC photoluminescence of these CDs is also observed [50]. In some cases, the solvothermal method is quite dangerous for those reactions occur violently and temperature rises too fast in limited reaction spaces which is horrible, leading to the explosion happen. To decrease the threatening to the laborotary and life, the conten of reactant and solvent should be as little as possible and the oxygen in solutions had better be excluded.

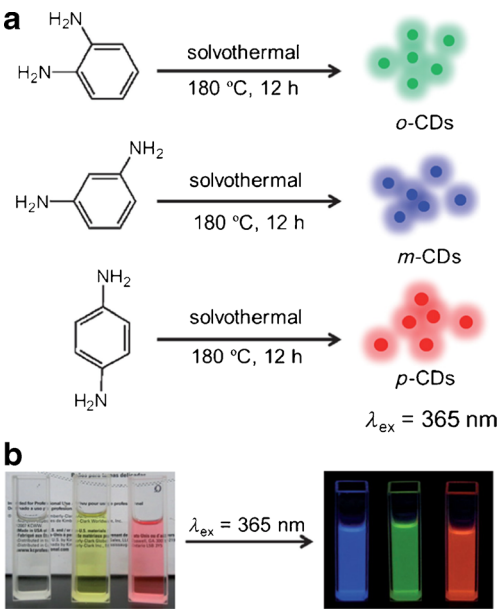

Fig. 5 **a** Preparation of the RGB (red, green and blue) PL X-CDs from three different phenylenediamine isomers. **b** Photographs of X-CDs from three different phenylenediamine isomers dispersed in ethanol in daylight (left), and under 365 nm UV irradiation (right). Produced with permission from ref. [50]

Microwave method

Herein, microwave method mainly refers to the synthesis of X-CDs by the assitant of microwave in the open systm without a sealed container neither high pressure. It is convenient and rapid to carbonize the precursors, so the synthesis process is simplified, obtaining the CDs within a few minutes and in a large amount. Doping of fluorescent CDs is achieved extensively by microwave method. Guan et al. explored nitrogen-doped CDs from folic acid molecules in a microwave method [51]. The CDs had a narrow size distribution. Moreover, it had low toxicity and was capable of labeling C6 cells. A microwave assisted synthesis of phosphorus- and nitrogen- codoped CDs from phytic acid and ethylenediamine as phosphorus and nitrogen sources separately were presented by Guan et al. (Fig. 6) [52]. The synthesized CDs showed high green fluorescence with quantum yield of 21.65% and cell-labeling ability, indicating great potential as bioimaging materials. By the similar way, uniform nitrogen and sulfur co-doped CDs were prepared by microwave treatment of citric acid and thiourea [53].

Surface functionalization

Surface functionalization is realized though surface functionalization of CDs with molecules containing heteroatoms. Surface functionalization with heteroatom is a powerful method to adjust the properties of CDs. According to the synthesis steps, surface functionalization methods can be mainly devided into multi-step synthesis and one-step synthesis. Some surface functionalization on modification methods, precursors, quantum yields, etc. are listed in Table 1.

Multi-step synthesis

Multi-step synthesis mainly consists the process of appearance of reactive groups and their modification through the surface chmistry, which usually causes a bit mor trouble yet is widely used for doping CDs with heteroatoms to reinforce their fluorescent property and meet the requirement of special applications.

Notably, the majority of CDs prepared by chemical oxidation, pyrolytic process are rich in oxygen- or amine- containing groups, which endows them with the ability in chemical bonding. Liao et al. reported the reversible fluorescence modulation of spiropyran-functionalized nitrogen-doped CDs [54]. In this work, fluorescent CDs with diameters of about 3 nm which can emit blue-green light were synthesized through the hydrothermal carbonization of ethylenediaminetetraacetic acid disodium salt. While the spiropyran-functionalized CDs centered at 510 nm can be switched off and turned on at 650 nm via energy transfer between the change of visible light irradiation and light irradiation, indicating that spiropyran-functionalized CDs may find potential applications in biological imaging and labeling, as well as individual light-dependent nanoscale devices (Fig. 7). Zheng et al. prepared a multifunctional theranostic C-dots by the conjugation of an anticancer agent oxidized oxaliplatin on the surface of C-dots [55]. The theranostic CDs successfully integrates the optical properties of CDs and the therapy performance of oxidized oxaliplatin, possessing good biocompatibility, bioimaging function, and anticancer effect. The in vivo results demonstrate that distribution of the drug can be monitored by the fluorescence signal of theranostic CDs. A novel CDs featuring efficient fluorescence resonance energy transfer (FRET) for two-photon photodynamic cancer therapy has been designed by Wang et al. [56]. A photosensitizer used for photodynamic therapy of cancers, were linked to CDs to form the conjugates nitrogen-doped CDs by the electrostatic force. The two-photon image of the nitrogen-doped CDs in Hela cells was clearly seen under the excitation of a femtosecond laser. The singlet oxygen production of the nitrogen-doped CDs was also much higher than that of the photosensitizer alone under two-photon excitation of a 700 nm femtosecond laser. These results demonstrate that the CDs and photosensitizer conjugates are promising for two-photon excitation photodynamic therapy of cancers and needed to investigate further.

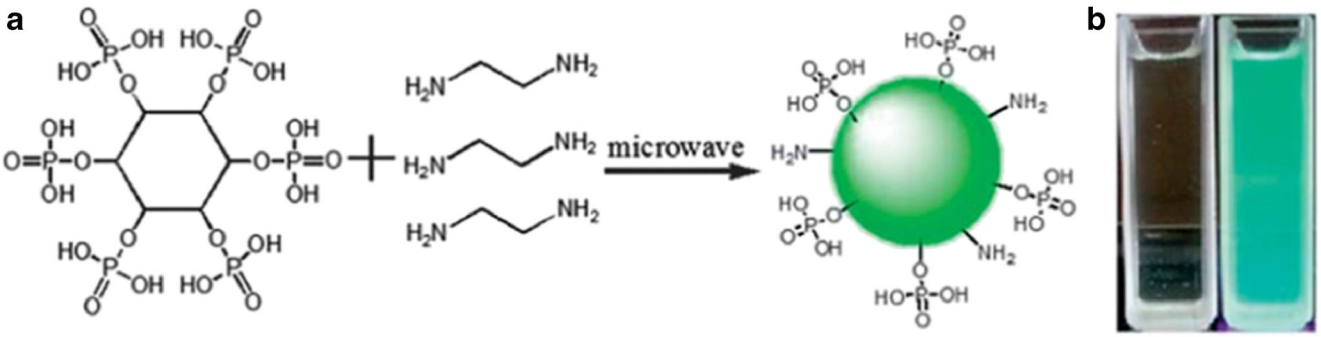

Fig. 6 **a** Schematic diagram for synthesizing phosphorous-doped CDs. **b** Emission under daylight and 365 nm ultraviolet excitation. Produced with permission from ref. [52]

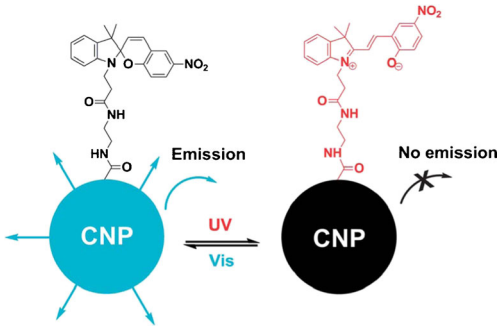

Fig. 7 Schematic illustration of light-induced fluorescence modulation of the spiropyran-functionalized CDs. Produced with permission from ref. [55]

In addition to molecular bonding to CDs, nanoparticles are also applied to decorate the surface of CDs. A simple and effective strategy for designing ratiometric fluorescent nanoprobe has been described by Liu et al. [57]. A CDs based dual-emission nanoprobe for Cu^{2+} detection was prepared by coating CDs on the surface of Rhodamine B-doped silica nanoparticles. The nanoprobe showed characteristic fluorescence emissions of Rhodamine B (red) and CDs (blue) under a single excitation wavelength. When Cu^{2+} was added, only the fluorescence of CDs was quenched, which led to the ratiometric fluorescence response of the dual-emission silica nanoparticles. This ratiometric nanoprobe exhibited was successfully applied for the ratiometric fluorescence imaging of Cu^{2+} in cells.

One-step synthesis

This kind surface functionalization is realized almost in one step to form the surface fanctionalized CDs through a top-down or bottom-up way, rather than synthesize raw CDs then functionalize them on the surface.

Size-controlled, amine-functionalized CDs were obtained from GO sheets, ammonia and hydrogen peroxide as starting materials [58]. In the synthesis process, hydrogen peroxide and ammonia cut GO sheets into smaller sizes and passivated the active surface separately and synergisticly to give amine-modified CDs (Fig. 8). These GQDs exhibited good antimycoplasma properties. Polyamine-functionalized CDs with high fluorescence quantum yield (42.5%) have been prepared by one-step carbonization of citric acid with branched polyethylenimine [59]. The obtained CDs are spherical graphite nanocrystals capped with abundant branched polyethylenimine at their surfaces, which suggests promising applications in chemical sensing.

All of the above summaries on synthetic strategies are categorized mainly depending on the characteristics of the ways of synthesis, and can't be distinguished absolutely. Sometimes, two or more synthetic strategies are applied comprehensively in synthesis to improve their optical and biological properties.

CDs doped with heteroatoms

As calculated by using density-functional theory (DFT) and time-dependent DFT calculations, the fluorescence of CDs is essentially originated from the quantum confinement of conjugated π-electrons in sp^2 carbon net work and doping foreign atoms is an effective way to tune the fluorescent properties of CDs. Various heteroatoms with different doping methods have been reported to adjust the properties of CDs. Some typical examples are listed in Table 2. We can see that the heteroatom's doping provides the possibility of modifying the PL properties of CDs in different aspects.

Nitrogen-doped CDs

Nitrogen-doping is the most studie way to modify the fluorescent properties of the CDs as the nitrogen atom has a comparable atomic side and five valence electrons for bonding with carbon atoms. Up to date, in the reports on the heteroatom-doped CDs, nitrogen-doping has taken up the most percentage both in quantity and type. In 2012, Li et al. made an attempt to synthesize nitrogen-doped CDs in an electrochemical approach for the first time by using nitrogen-contiaining tetrabutylammonium perchlorate in acetontrile as the electrolyte to introduce nitrogen atoms in the CDs facilely, which showed unique optoelectronic features [39]. Accordingly, Zhang et al. presented an electrochemical method for synthesizing uniform sized graphene quantum dots with a yellow emmision on a large scale [40].

In the process of oxidation or decomposition with strong oxidizing acid HNO_3, nitrogen would be doped into the CDs. However, just this is not enough, because the obtained CDs are poor in nitrogen with short emission (blue or green colour) and low fluorescent quantum yield, making them difficult to use in applications [19, 24, 61]. So the further functionalization is required. For example, Choi et al. described a novel design of highly biocompatible CDs for simultaneous bioimaging and targeted photodynamic therapy in vitro and in vivo. As expected, the initial nitrogen-doped CDs obtained through HNO_3 has poor fluorescent properties. After subsequent functionalization with folic acid, the new nitrogen-doped CDs with improved fluorescent properties can serve as carriers for the photosensitizers zinc phthalocyanine, offering a convenient and effective platform for enhanced photodynamic therapy to treat cancers in the near future [62]. An exception was reached by Shao et al., who applied a high concentration nitric acid oxidation strategy for one-step fabrication of highly red-emitting fluorescent nigrogen-doped CDs using activated carbon as a carbon

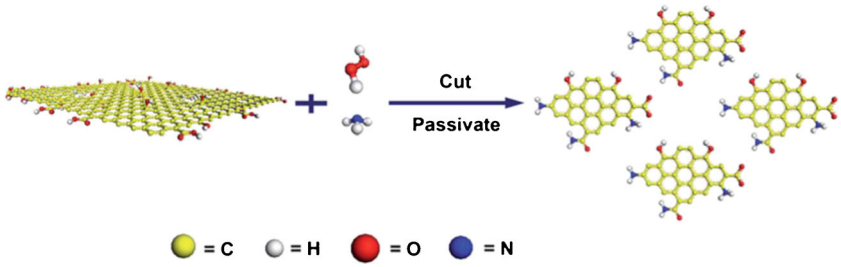

Fig. 8 Illustration of the preparation of amine-functionalized CDs. Produced with permission from ref. [58]

Table 2 Information of partial CDs doped with various types of hetetoatoms

Types	Particle Size (nm)	Ex/Em (nm)	Decay Time (ns)	QY (%)	ZP (mV)	UC	Ref.
Nitrogen	5–10	360/540	–	14	-48	–	40
	6.8	360/466, 450/555, 540/637	3.20, 0.87, 0.68	11.9, 16.7, 26.2	–	–	49
	6.0, 8.2, 10.0	–/435, 535, 604	4.44, 0.99, 9.39	10.4, 4.8, 20.6	–	Yes	50
	3	340/425	–	–	–	–	35
	4.5	360/450	1.55, 4.13, 5.52	7.8–10.9	-39.8	–	62
	3.3–12	520/600	–	50	–	–	63
	3	390/520	6.27	31	-21	Yes	64
	2.6–3.8	368/475	7.26	18–45	–	–	65
	2.63	330/483	–	16.5, 25.66	–	Yes	128
Phosphorus	5–15	372/408	5.0	25.1	–	–	8
	3–5	370/470	–	11.0–19.7	-22.1	–	67
Sulfur	3.0	380/480	5.8	10.6	–	–	43
	1–2	340/446	1.15	11.8	-42.7	–	70
	10	–/640	–	2.3	-27.33	–	71
	11.8	375/500	1.96	–	–	–	72
Selenium	1–5	467/563	3.44	29	–	–	76
Silicium	7	300/382	3.3	19.2	–	–	77
	12	360/450	–	47	–	–	78
Boron	3	310/440	–	–	–	–	80
	4	320/430	–	21.1	–	–	81
	8–22	315/368	–	14.8	–	–	82
	2–6	350/450	5–10	10–15	–	–	83
	3–7	400/523	–	3.6	–	Yes	42
	3–5	360/535	–	5	–	–	12
Fluorine	3–10	330/445	4.45	7.5	-10	–	87
Chlorine	3–5	310/440	8.4	3.4	–	–	86
Bromine	3–5	233/417	3.8	0.5	–	–	86
Iodine	3–5	232/449	2.9	1.7	–	–	86
N & S	3.1	340/430	13	71	–	–	88
	2.78	369/444	7.88	14.5	–	–	89
	2.8	318/403	14.01	27.2	17.6	–	90
	2.88	430/522	7.65	31.67	–	–	53
	5.24	320/432	5.4	18.6	–	–	91
N & P	5–10	225/453.4	–	6.3	8.86, −0.02	–	92
	2.06	460/525	0.44, 1.62	27.5	–	Yes	93
	4.11	420/500	2.7	16.8	12.8	–	94
	3–5	370/470	–	11.0–19.7	-14.7, −22.1	–	67

source, endowing their promise as a potential near-infrared fluorophore for bioimaging [63].

As nitrogen-doping is an efficient way to tune the fluorescent properties of CDs, more and more innovative works are being reported. For instance, Liu et al. reported the biocompatible nitrogen-doped CDs as efficient two-photon fluorescent probes [64]. The nitrogen-doped CDs was prepared through a one-pot solvothermal approach at high temperature of 200°C using GO as precursor and DMF (N,N-dimethylformamide) as a solvent and source of nitrogen (Fig. 9). The decomposed dimethylamine was doped into the GO through nucleophilic ring-opening reaction with the epoxy group on the surface of GO. The two-photon-induced fluorescence of CDs with a two-photon absorption cross section and large imaging penetration depth was systematically investigated using near-infrared laser as excitation and applied for efficient two-photon cellular and deep-tissue imaging. Wang et al. reported the gram-scale synthesis of nitrogen-doped CDs with single-cystalline by a facile molecular fusion route under mild and green hydrothermal conditions [65]. As the precursor, cheap and low-toxicity pyrene was nitrated into trinitropyrene in hot HNO_3 under refluxing. After alkalization, the suspension was hydrothermally treated and dialysed to prepare the nitrogen-doped CDs, where alkaline species play an important role in tuning their size, functionalization, and optical properties. Compared to the multistep organic-phase fusion, the water-phase fusion is much more milder, simpler, greener, lower in cost and higher in overall product yield. The single-cystalline CDs are bestowed with bright excitonic fluorescence, large molar extinction coefficents and long-term photostability, exerting a great impact on fluorescence microscopy for clinical diagnostic applications.

Phosphorus-doped CDs

Notwithstanding phosphorus atom is larger than carbon atom, it has been indicated that phosphorous can come into being substitutional defects in diamond sp^3 thin films, serving as an n-type donor and therefore tuning the optical and electronic properties [66]. In the light of the unusual quantum-confinement and edge effects of CDs, doping with phosphorous atoms results in the presence of more active sites and alters their electronic characteristics, thus offering novel and unexpected fluorescent properties. Zhou et al. presented an efficient method to synthesize phosphorous-doped CDs through solvent-thermal reaction between phosphorous bromide and hydroquinone under 200°C in a Teflon-lined vessel, presenting strong blue fluorescence with quantum yild up tp 25% [8]. Compared with undoped CDs, phosphorous CDs have larger size and improved emission efficiency. Sarkar et al. synthesized phosphorous-doped CDs with the assistant of NaH_2PO_4 by heating in a furnace. The doping of phosphorous to these CDs improved their fluorescence intensity as well as quantum yileds [67].

Sulfur-doped CDs

Sulfur atom is larger than carbon atom to a great extent. What's more, the difference of electronegativity between sulfur (2.58) and carbon (2.55) is so small that the significant charge transfer in carbon and sulfur seems scarely possible [68], thus the chemical dopoing of sulfur into CDs would appear to be rather challenging [69]. Chandra et al. have developed a facile route to synthesise sulfur-doped CDs for the first time without surface passivation, exhibiting a wide band

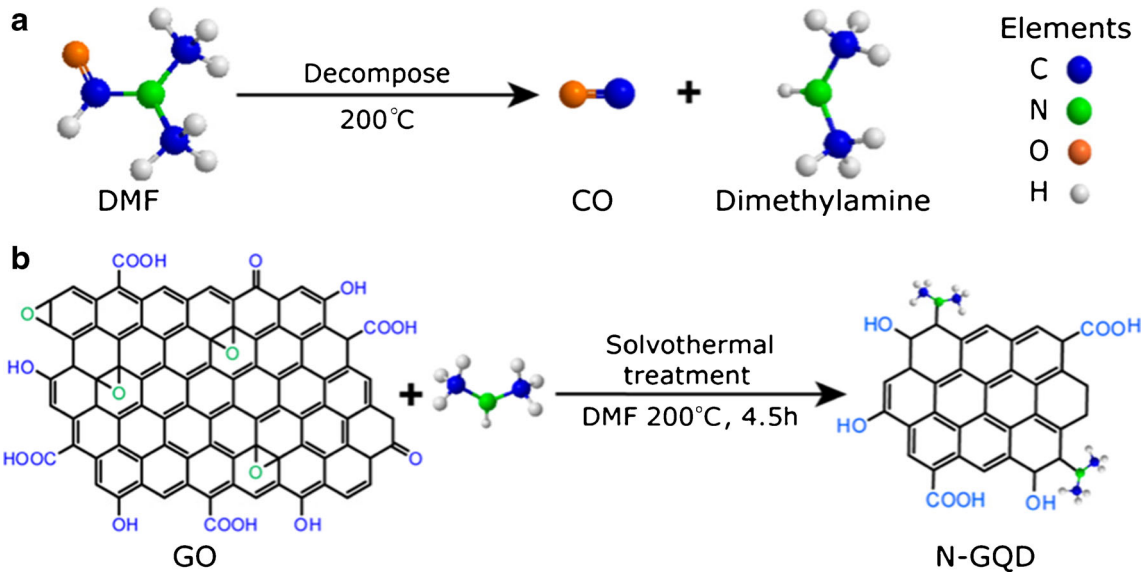

Fig. 9 **a** Decomposition of DMF at a high temperature. **b** Schematic illustration of the strategy for the nitrogen-doped CDs (N-GQD) preparation. Produced with permission from ref. [64]

gap of 4.43 eV with a high open circuit voltage of 617 mV. This kind of sulfer-doped CDs was prepared with precursor first through reflux in the presence of concentrated sulfuric acid and then by polymerization in a vacuum oven. Such synthetic CDs present good water dispersibility, high photostability and negligible toxicity and exhibit bright blue fluorescence, having the potential to act as an excellent bioimaging agent and drug delivery vehicle [70]. The graphite rod as a working electrode was inserted into sodium *p*-toluenesulfonate aqeous solution. After electrochemical reaction, the sulfur-doped CDs was collected and dialyzed, which was successfully applied to the biochemical analysis as novel fluorescent probe. Ge et al. has promoted progressive development of sulfur-doped CDs to a large extent [71]. The precursor molecule polythiophene phenylpropionic acid was first prepared by means of oxidative polymerization. Then, using the hydrothermal method, the polymers were carbonized to form sulfur-doped CDs, which have exceptional such as broad absorption, activity in photoacoustic imagine, high photothermal conversion efficiency of 38.5% and visible light excitaion. Up to date, the obtained sulfur-doped CDs is the first red emissive CDs that can simultaneously serve as fluorescent, photoacoustic and thermal theranostics for cancer diagnosis and treatment in living mice, thereby significantly broadening the biomedical application of CDs. While Park et al. developed a versatile platform using block copolymer-integrated CDs (a kind of sulfur-doped CDs, Fig. 10) for highly efficient, colorimetric mutifunctional sensors, which showed simultaneous sensing behavior to temperature, pH and metal ions [72]. The detailed mechanism of the response of the sulfur-doped CDs was elucidated by time-resolved fluorscence and dynamic light scatering.

Selenium-doped CDs

Selenium-doping has ignited increasing interest in reversible fluorescent probes for real-time imaging of redox status changes in biosystems as selenium plays a vital role as the active site of the antioxidant enzyme glutathione peroxidase [73–75]. However, to the best of our knowledge, selenium-doped CDs have rarely been reported. Yang et al. designed a new reversible fluorescent swich for the detection of oxidative hydroxyl radical and reductive glutathione based on the use of selenium-doped CDs [76]. The selenium-doped CDs were pepared hydrothermal treatment of NaHSe aqueous solution containing graphene oxide quantum dots. The C-Se group in selenium-doped CDs can be oxidized by hydroxyl radical to a nonfluorescent Se-Se group, and the Se-Se groups can be effectively and rapidly reduced to C-Se group through glutathione, which constitutes a reversible on-off fluorescent swich (Fig. 11).

Silicium-doped CDs

Silicium, which belongs to the same group as carbon, group IV, and prefers sp^3-like bonding, is considered to influence the

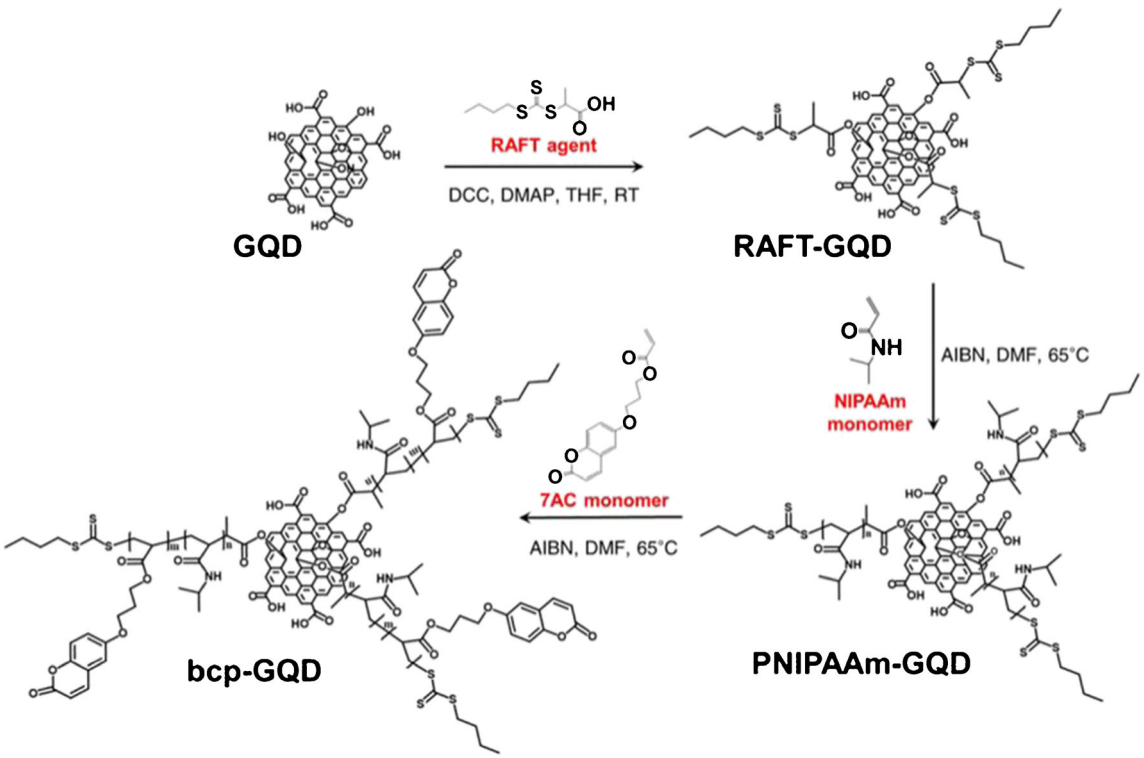

Fig. 10 Synthesis of bcp-GQD (a kind of sulphur- doped CDs). Produced with permission from ref. [72]

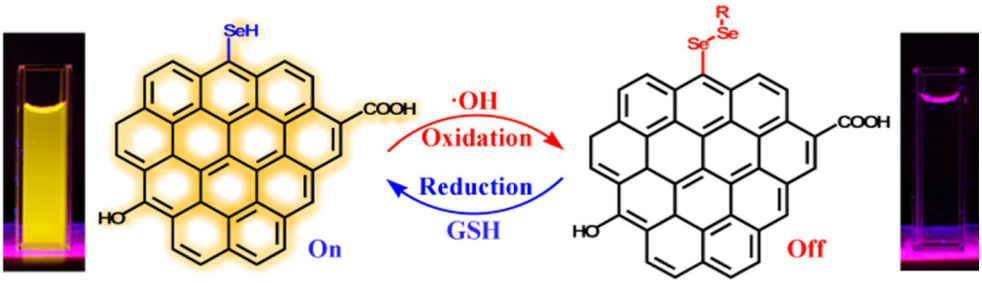

Fig. 11 Synthesis of bcp-GQD (a kind of sulphur- doped CDs). Produced with permission from ref. [76]

electronic and structural properties of CDs when it is applied in doping [77]. Wang et al. firstly reported the use of an organosilane as a coordinating solvent to synthesize highly fluorescent silicium-doped CDs in one minute [78]. The synthesis proceeds via pyrolisis of citric acid in N-(β-aminoethyl)-γ-aminopropyl methyldimethoxy silane at 240°C for 1 min, which is fascinating with the low cost, high boiling point, excellent chemical stability and rich available functional groups. The silicium-doped CDs, which benefit from surface methoxysilyl groups, have a relatively smaller diameter of 0.9 nm and can be manufactured into CDs fluorescent films or monoliths. The heteroatom-doped CDs synthesized by this novel way would encourage their research in medical diagnostics. Qian et al. presented an efficient route to fabricate silicium-doped CDs with strong photoluminescence through a solvent-thermal reaction using $SiCl_4$ as the silicium source and hydroquinone as the carbon precursor [77]. Based on the remarkable quantum-confinement and edge effects of CDs, doping CDs with silicium alters their electronic characteristics, thus producing unexpected properties. Specific electron transfer between silicium-doped CDs and hydrogen peroxide provides a sensitive fluorescence sensing platform for hydrogen peroxide.

Boron-doped CDs

The boron atom has similar atomic radium though fewer valence electons. A boron-carbon bond is 0.5% longer than that of a carbon-carbon bond and tends to cause a certain extent of chemical disorder [79], so doping CDs with boron would alter their optical properties and offer more active sites, thus rendering new phenomena and novel applicaions.

Zhang et al. presented a hydrothermal approach for the cutting of boron-doped graphene into boron-doped CDs [80]. They first prepared boron-doped graphene through graphene sheets in the presence of boron oxide, then synthesized boron-doped CDs from boron-doped graphene by a hydrothermal approach. The presence of boronic acid groups on the CDs surface helps their application as a new fluorescent probe for glucose sensing. It is postulated that the interaction between the *cis*-diol groups in glucose and the boronic acid groups on the CDs surface forms structurally rigid aggregates, restricting the intramolecular rotations and thus producing a great fluorescence enhancement. In the top-down strategy, Hai et al. prepared boron-doped CDs via a one-pot microwave approach with graphene oxide as the carbon source and borax as the boron source (Fig. 12) [81]. The microwave preparation method not only significantly reduces the reaction time, but also avoids the use of strong oxidizing acids. The incorporation of boron atoms into CDs offer them with excellent fluorescent stability in a wide pH range, favorable capability for anti-photobleaching and high tolerance to external ionic strength.

In view of bottom-up strategy, Shan et al. fabricated boron-doped CDs by using BBr_3 as the boron source and hydroquinone as the precursor via one-pot solvothermal route [82]. Based on the effective fluorescence-quenching effect by charge transfer of doped boron atoms with hydrogen peroxide, a boron-doped CDs-based fluorescence analytical system for hydrogen peroxide was constructed. Bourlinos et al. synthesized boron-doped CDs by microwave heating of an aqueous solution of citric acid, boric acid and urea with ultrafine size and quasi-spherical shape [83]. The boron-doped CDs exhibit apparently higher nonlinear optical response than other similar CDs.

Electrochemical exfoliation method is applied into the preparation of boron-doped CDs extensively. Fan et al. demonstrated that boron-doped CDs exhibited rich fluorescence owing to their special interaction with the surrounding media [42]. The electrolysis of graphene rod was performed on CHI 705 electrochemical workstation, in which borax was used as electrolyte. The boron-doped CDs were improved to be a biomarker for cellular imaging and electrocatalysis for oxygen reduction. Cai's group synthesized boron-doped CDs by oxidizing a graphite rod in aqueous borax solution with a Pt cathode at a constant voltage of 3 V, which was performed on a CHI 660B electrochemical workstation [12]. The obtained boron-doped CDs emit a strong fluorescence and the fluorescence intensity is directly related to the amount of hematin, offering a new practical tool for clinical examinations and diagnoses.

Halogen-doped CDs

Halogen has been used to modulate the optical properties of carbon nanotubes and grphene [84, 85]. In this sense,

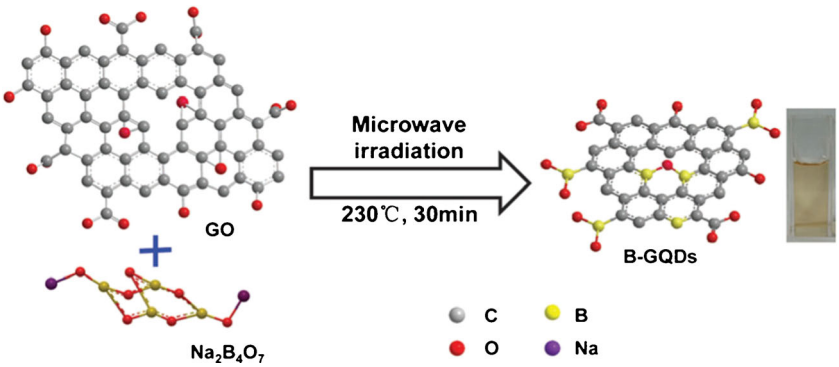

Fig. 12 Preparation scheme for the boron-doped CDs (B-GQDs) by using GO and borax as carbon and boron sources. Produced with permission from ref. [81]

halogenation may be a good option to alter fluorescent properties of CDs. Zhou et al. prepard halogenated CDs which were doped with chlorine, bromine and iodine seperately through solvent-thermal reaction in a simple and efficient method, and provided an alternative approach for further functionalization of CDs [86]. Sun et al. developed a strategy through combining a microwave-assisted technique with hydrothermao treatment to improve production yield of fluorine-doped CDs prepared by top-down methods. By using fluorinated GO as a raw material, fluorine-doped CDs can be synthesized. Moreover, doping with florine improves the pH stability of photoluminescence [87]. At the same time, as fluorine with strong electron-withdrawing property reduces the π-electtron density of the aromatic structure, the reactivity to singlet oxygen is inhibited and thus the photostability is improved.

Codoped CDs

Codoping CDs with dual heteroatoms has been emerging as a hot research top out of curiosity. As mentioned above, nitrogen-doping is widely used in preparation of heroatoms-doping of CDs. In the codoping of CDs, nitrogen is one of the most used elements. The codoping of CDs can be mainly classified to two kinds in terms of the kinds of heteroatoms, which is nitrogen and sulfur codoped CDs and nitrogen and phosphorous codoped CDs.

In the bottom-up strategy, nitrogen and sulfur codoped CDs were developed by using citric acid as the carbon source and thiourea as nitrogen and sulfur sources. Qu et al. dissolved citric acid and thiourea into water and then transferred them into a Teflon lined stainless autoclave to hydrothermally synthesize nitrogen and sulfur codoped CDs which showed high quantum yield of 71%, excitation independent and single exponential decay [88]. Taking advantage of the same precursors, Feng et al. prepared nitrogen and sulfur codoped CDs by thermal treatment at 200°C for 2.0 h, which is used for bioimaging with improved biocompatibility [89, 90]. When the precursors citric acid and thiourea met the microwave treatment by the same research group, the nitrogen and sulfur codoped CDs showed excitation wavelength and pH dependent fluorescence behavior in the visible range [53]. Zhang et al. fabricated nitrogen and sulfur codoped CDs via a one-step hydrothermal method using GO in a top-down strategy [91]. Ammonia and powered S were selected as the source of nitrogen and sulfur, respectively (Fig. 13). The codoped CDs displayed amazing enhancement fluorescence when compared with only nitrogen-doped CDs and excellent fluorescent stability at high salt concentration.

Nitrogen and phosphorous codoped CDs have also been researched in some works. Using a facile one-pot microwave-assisted process, Prasad et al. synthesized a kind of CDs with metal-free nitrogen and phosphorous codoped, electrocatalytically active and photoluminescent CDs by employing DMF and phosphoric acid as precursors, which paves the way for photoluminescent CDs that can be used in light-emitting diode, drug delivery and cellular imaging [92]. Ananthanarayanan et al. demonstrated a simple strategy for the synthesis of nitrogen and phosphorous codoped CDs from a single biomolecule precursor adenosine triphosphate (ATP) [93]. ATP powder was first carbonized by heating in a quartz tube furnace at 900°C for 1 h, followed by refluxing in HNO_3 for 24 h. Such nitrogen and phosphorous codoped CDs exhibit

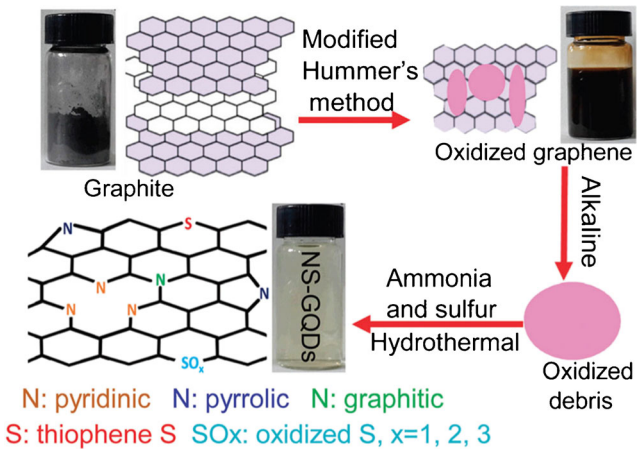

Fig. 13 Schematic and digital photos of nitrogen and sulphur codoped CDs (NS-GQD) preparation. The location and chemical state of N and S in NS-GQDs. Produced with permission from ref. [91]

good two-photon excitation properties (absorption cross-section as high as 20,000 GM). Liu et al. prepared nitrogen and phosphorous codoped CDs by hydrothermal treatment of glucosamine with excess pyrophosphate, offering constant green fluorescence emission at different excitation wavelengths and high stability when exposed to different pH and ionic environments [94]. Sarkar et al. synthesized nitrogen and phosphorous codoped CDs in multi-steps [67]. They first synthesized amino acid funcionalized CDs in a bottom-up approach with citric acid, amino acid and NaH_2PO_4 as the sources of carbon, nitrogen and phosphorous respectively.

Properties and fluorescent mechanism

Methods for particle characterization

For the sake of obtaining the information about the phycial and chemical properties of X-CDs, many modern analysis and testing technologies are applied in characterizing CDs, such as transmission electron microscope (TEM), atomic force microscope (AFM), X-ray diffraction (XRD), fourier transform infrared spectroscopy (FTIR), X-ray photoelectron spectroscopy (XPS) and Raman spectroscopy.

TEM has a ralatively high resolution of upto 0.1 ~ 0.2 nm, so samples can be observed with a magnitude of enlargement from tens of thousands to millions of times and the ultrastructure of the samples can also be found. TEM is extensively used in the research of CDs. To observe the fine-structure of CDs, the function of high-resolution transmission electron microscopy (HRTEM) is usually applied. A structural characteristic of CDs is that the lattice fringes of crystalline nature can be divided into two kinds, namely (002) interlayer spacing and (1120) in-plane lattice spacing, respectively. The former usually centered at about 0.34 nm, which can be found from nitrogen-doped CDs prepard by hydrothermal treatment of carbon black [95], while the latter mostly centered at about 0.24 nm can be found from nitrogen-doped CDs prepared via soverthermal-treatment of small molecular precursors [96].

AFM is a type of scanning probe microscopy, with demonstrated resolution on the order of fractions of a nanometer. The information is obtained by "touching" the surface with a mechanical probe [97]. The thickness and height distribution of heteroatom-doped CDs can be characterized by AFM after the deposition of the CDs onto a plasma-treated Si wafer or freshly exfoliated mica, drying under ambient conditions [98–101]. For example, if a typical topographic height is less than 1.4 nm, the heteroatom-doped CDs generally contain 3–4 layers of graphene sheets (Fig. 14) [102], as a single graphene layer is usually has a thickness less than 0.5 nm.

XRD is a tool used for identifying the atomic structure of a cystal in heteroatoms doped CDs. By measuring the angles and intensities of diffracted beams, the mean positions of the

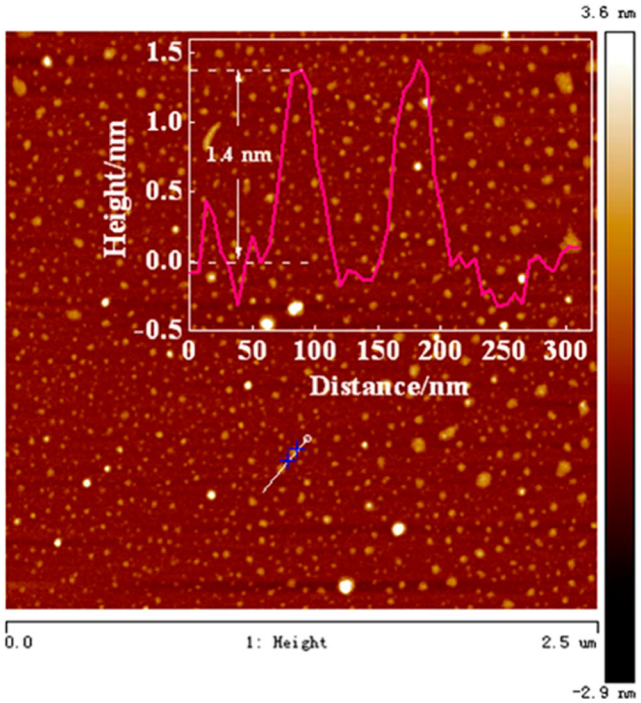

Fig. 14 AFM image of nitrogen-dope CDs; inset: height profile. Produced with permission from ref. [102]

atoms can be determined, as well as their chemical bonds, their disorder and various other information [103]. Heteroatoms doped CDs usually exhibits a peak around 26° as one prominent peak corresponding to (002), which represents a graphitic structure of heteroatoms doped CDs. However, the peak of heteroatoms doped CDs is weaker and broader compared with graphite due to the thinness, disordered stacking and the introduction of heteroatoms of CDs [104–107]. What's more, the changes of peaks at around 26° and 13.4° represent the interplaner graphitic stacking and in-planer structural packing respectively, reflecting the formation of heteroatoms doped CDs [89–107].

FTIR is a technique which is often used to obtain an infrared spectrum of absorption of emission of heteroatoms doped CDs by collecting high spectral resolution data over a wide spectral range simultaneously. For example, in nitrogen-doped CDs, the characteristic absorption bands of N-H stretching vibrations can be observed between 3440 cm^{-1} and 3200 cm^{-1} and N-H bending vibration is at about 1583 cm^{-1}; C = N stretching vibrations can be found in the range of 2000 cm^{-1} to 1650 cm^{-1}; while C-N stretching vibration is between 1420 cm^{-1} and 1340 cm^{-1} [108–110]. In the spectrum of phosphorous-doped CDs, peaks at 1128 cm^{-1}, 1055 cm^{-1}, 972 cm^{-1} and 950 cm^{-1} are attributed to the vibration of P = O, P-R, P-O-H and P-N respectively [51, 92]. For the sulfur-doped CDs, the peak in the range of 2568 cm^{-1} and 2380 cm^{-1} is ascribed to the stretching vibration of S-H group; the featured peaks of 1096 cm^{-1} and 635 cm^{-1} is due to the stretching vibrations of S = O and S-C respectively; the

stretching vibrations of thiocarbonyl group (C = S) present at around 1072 cm^{-1} [70–72, 91, 94]. In the silicium-doped CDs, the peak around 1060 is originated form the Si-O-Si asymmetric stretching, and the vibrational peaks at 793 cm^{-1} and 455 cm^{-1} are assigned to the Si-O bond [78, 111]. Note that the peak at 1450 cm^{-1} to 1405 cm^{-1} is the asymmetric stretching vibration mode of B-O; the stretching vibration bands of B-C appear at about 1138 cm^{-1} to 1190 cm^{-1} [12, 80, 81, 83]. And a shoulder vibrational peak of -C-F at 1200 cm^{-1} was collected for fluorine-doped CDs [87].

XPS characterization is in common use to explore the chemical composition and configuration of X-CDs almost without any exception as it is a powerful surface-sensitive quantitative spectroscopic technique that measures the elemental composition, chemical state and electronic state of the elements within CDs. In the wide-scan of survey spectra, every peak represents a kind of element. Before beginning the process of peak identification, charge referencing of carbon and oxygen is needed to obtain meaningful binding energies (BEs). BEs that identify the shell and spin-orbit of each peak produced by a given element can be consulted in various handbooks [112]. Even though the elemental composition is unknown, the characteristic BEs of special elements can be identified. By reading the wide scan of CDs, we can pick up the information of heteroatoms being contained in CDs qualitatively and quantitatively. Through peak-fit process of high energy resolution XPS spectra, which is full of art, science, knowledge and experience, the information of chemical state and electronic state of the elements can be obtained. For instance, Ji et al. studied the detailed surface composition and bonding information on the doped boron atom in the CDs by XPS spectra, which indicated the presence of B, C and O elements and corresponding B 1 s, C 1 s and O 1 s peaks at about 191, 284 and 531 eV (Fig. 15a), respectively, confirming the doping of boron into the raw materials [12]. The high resolution XPS peaks of C 1 s (Fig. 15b) and B 1 s (Fig. 15c) indicate the presence of C-B, BC_2O, BCO_2, agreeing with the results from the FTIR spectrum and further confirming the doping of boron into the CDs. The high-resolution N 1 s spectrum of the N-GQDs can reveal the presence of pyridine-like (397.8 eV), pyrrolic (399.4 eV) and amino (401 eV) N atoms [37, 102, 113]. To the best of our knowledge, there has no report on separating different states of doped element and researching their effects on the fluorescence of X-CDs while related researches are mentioned in some works. Chen et al. demonstrated that non-linear emission from CDs could arise when electron-withdrawing NO_2 and electron-donating NH_2 groups at the edges forms a donor-GQD-acceptor system [93]; and Qian et al. showed that the quantum yields of X-CDs doped with different diamines do not correlate with

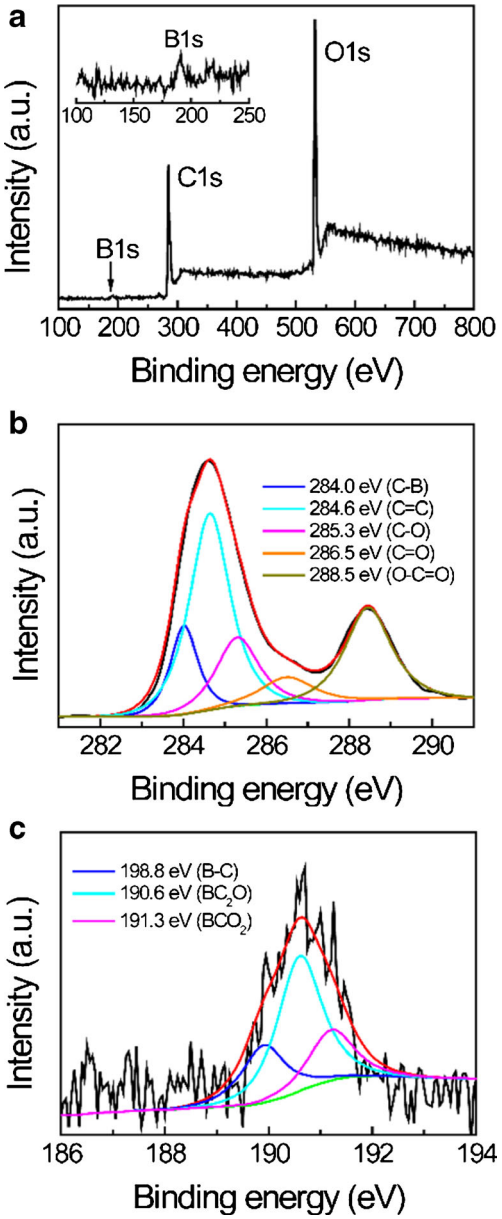

Fig. 15 **a** XPS wide-scan spectrum of boron-doped CDs. The inset shows the amplified XPS of B 1 s. **b**, **c** High-resolution XPS spectra of C 1 s and B 1 s in CDs, respectively, and their related curve-fitted components. Produced with permission from ref. [12]

the nitrogen content which may be from different ratios of pyridinic to pyrolic nitrogen atoms in those X-CDs and only pyrolic nitrogen atoms can take part in the protonation process to enhance the fluorescence of X-CDs [113].

Raman spectroscopy is also a powerful and non-destructive tool for the characterization of X-CDs. In the Raman spectrum, two remarkable peaks at around 1360 and 1590 usually appear, corresponding to D band and G band respectively. The G band is assigned to the E_{2g} vibration modes of the sp^2 carbon domains, explaining the degree of graphitization. The D band arises from structural defects and partially disordered structures of sp^2

domains. Traditionally, the intensity ratio of disorder D to crystalline G (I_D/I_G) is used to evaluate the disorder in CDs. The I_D/I_G values of CDs may be quite various depending on the preparation methods. In Hai's microwave approach, the I_D/I_G ratio of boron-doped CDs (1.04) is lower than that of GO (1.12), indicating that the disorder degree of boron-doped CDs is reduced with respect to GO (Fig. c) [81]. While the value of the ratio is 0.94, which is higher than that for pristine graphene (0.79), suggesting a breakage of the graphene due to the boron-doping [12].

Zeta potential

The zeta potential (ZP) is a kind of important indicator of feasibility for the formation of a stable particle dispersion of heteroatoms doped CDs and their magnitude indicates the degree of electrostatic repulsiont between CDs in a dispersion. After doping with heteroatoms, the ZP of CDs vary significantly according to the synthetic routes used and pH solution, and not all doping methods can improve the ZP notably [114]. Some more meaniful results are reported with regard to the dispersion and stability of CDs. Liu's nitorgen-doped CDs solution has a potential of −21 mV in water, which shows a transparent homogeneous phase without any agglomeration for at least 20 months [64]. The suspention of nitrogen-doped CDs prepared by Choi et al. is highly stable, with a ZP of −39.8 mV [62]. The X-CDs made via the electrochemical method are highly negatively chareged with ZP up to −48 mV and strong electrostatic repulsion, forming stable aqueous solution. The abundant charged surface impart sufficent colloidal stability to the X-CDs.

Fluorescence properties

From fundamental and application-oriented perspective, one of the most fascinating featurs of CDs is their fluorescence properties arising from quantum confinement effects.

Spectra

X-CDs with different color from blue to red have been synthesized and most common are blue and green, which in many cases show wide emission spectra due to the hetetogeneity in chemical composition and size. Usually, the fluorescence intensity maximum red-shifts as the excitation wavelength increases, exibiting excitation dependent emission wavelength and intensity [19]. As shown in Fig. 16, the fluorescence spectra of nitrogen-doped CDs show excitation shifts by changing the excitation wavelength from 310 to 390 nm, along with a notable change of the fluorescenc intensities [92]. CDs have only one maximum emission which is excited by the only maximun excitation. The excitation-independent fluorescence behavior has also emerged, which may be attributed to their

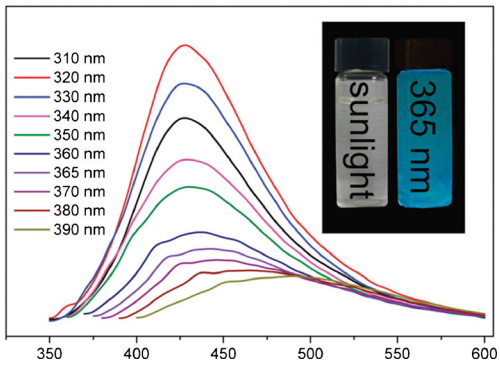

Fig. 16 Fluorescence spectra of a kind of nitrogen-doped CDs at different excitation wavelengths. Inset are digital photos of nitrogen-doped CDs. Produced with permission from ref. [92]

uniform size and surfac chemistry [42], and the intensity of fluorescence increased to the maximum and then decreased (Fig. 17). Generally, the emission spectra of CDs are symmetrical in the main, with large Stokes shifts as compared with that of organic dyes [115].

Quantum yields

Doping is an effective way to improve the fluorescence quantum yields (QY) in order to meet the requirements in bioimaging because of the introducton of emissive energy traps to facilitate the emissive recombination of localized electron-hole pairs [22]. When CDs were first discovered, their QY is lower than 1%. After doping with heteroatoms, the QY can be increased dramatically [24]. Doping can reduce and replace the carboxyl and epoxy groups in CDs, and enhance the fluorescence intensity because these groups can lead to non-radiative recombination [25]. For example, Li et al. prepared highly luminescent nitrogen-doped CDs, displaying a quantum yield of 16% [116]. A kind of nitrogen and sulfur codoped CDs reported by Guo et al. has s high QY of 10% [117]. The nitrogen and phosphorous codoped CDs prepared by microwave-assisted thermalysis of N-phosphonomethyl aminodiacetic acid and ethylenediamine show a quantum yield of 17.5% [118]. Rong

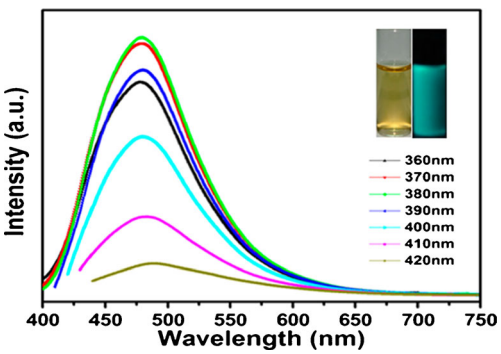

Fig. 17 Fluorescence spectra of a kind of sulphur-doped CDs at different excitation wavelengths. The inset are the photographs of the sulphur-doped CDs queous solution under visible light (left) and a UV beam of 365 nm (right). Produced with permission from ref. [43]

et al. sythesized nitrogen and phosphorous codoped CDs, exhibitting almost the highest QY of 90.2% [39].

Decay times

Fluorescence spectroscopy is extended by time-resolved fluorescence spectroscopy which uses convolution integral to calculate a lifetime and study the fluorescene properties. Fluorescence decay showed that X-CDs by many methods have multiexponential fluorescence decays [69, 103, 119, 120]. The multiexponential nature of the lifetime indicates the presence of multiple radiative species and different emissive sites [121]. The mean lifetime is calculated to be around several ns; such a short lifetime indicates that the fluorescence mechanism is possibly the redioactive recombination of excitaions [42, 104]. And from the view of short lifetime, ultrasmall sized X-CDs can also be identified as an aromatic macromolecule [64] and suitable for bioimaging [93]. Experimets prove that the larger the diameter of the X-CDs, the shorter the average lifetime. In Ke's report, the average fluorescence lifetime was shortened from 3.37, 2.75, 1.98 to 1.07 ns with an increase in size of nitrogen-doped CDs from 2 to 3, 2–5, 4–8 to 5–10 nm, respectively (Fig. 18) [122]. This size-dependent optical properties are mainly attributed to the quantum confinement effect. According to the lifetimes, it can be inferred that the photoluminescence of X-CDs belongs to fluorescence [8, 123]. In the presence of analyte, the life time of X-CDs as a on-off probe may decrease, revealing that the quenching mechanism is a dynamic quenching mechanism [89, 124]. In the doping by linking organic dyes to CDs, the decrease in fluorescence lifetime can provide additonal evidence of the fluorescence resonance energy transfer process [125]. Using the same CDs as precursors, the obtained X-CDs may have close lifetimes [91]. It should be mentioned that for the X-CDs, monoexponential decay is also discovered, and the superior optical characteristics is well correlated with the high-quality features of the CDs such as being uniform in size, almost defect-free single-crystalline structure and ideal electron-donating functionalization at edge sites [65, 88].

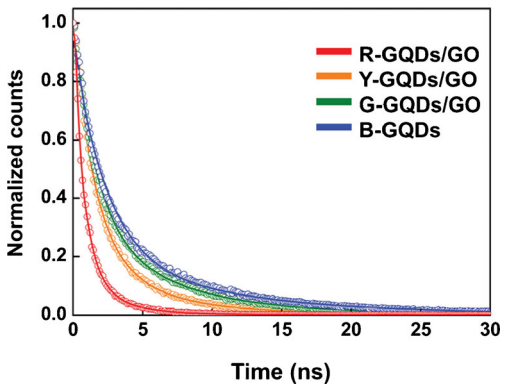

Fig. 18 Time-resolved fluorescence decays of CDs with different colour. Produced with permission from ref. [122]

UC properties

Photon UC is a process in which the sequential absorption of two or more photons (e.g. near infrared light (NIR)) leads to the emission of light at shorter wavelength (e.g. visible light) than the excitation wavelength [126]. It is an anti-Stokes type emission. The UC materials as fluorescent probes have many advantages for probing biolocial activities deep inside living organisms as they benefit from reduced photodamage, improved tissue penetration depth and a high signal-to-noise ratio due to the minimized autofluorescence background generated by NIR excitation. The UC X-CDs for fluorescence imaging have drawed much atttention for its promising applications in both biological research and clinical diagnostics [64]. For example, early diagnosis of tumor malignancy is crucial for timely cancer treatment, in which UC-based bioimaging can overcome the limitations of low tissue penetration and background autofluorescence from traditional fluorescence-based imaging as their excitation occurs at lower frequencies and the emission at higher frequencies [127].

Up to date, more and more X-CDs with UC properties have been emerging as a new member of UC materials family. However, the exact up-conversion mechanism of heteroatom-doped CDs is still an enigma though many groups have tried to uncover the origin through different methods. There are different reviews concerning the explanation for this phenomenon. Zhang et al. found that their nitrogen-doped CDs showed efficient UC emission when excited using long-wavelength light. Considering that the energy difference between the excitation light and emission light in the UC process is not fixed, they speculated the multiphoton active process for explaining UC emission of the nitrogen-doped CDs (Fig. 19) [108]. Cui et al. reported a method to simultaneously enhance the UC

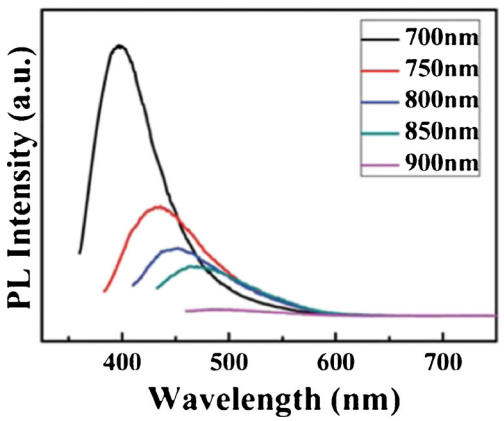

Fig. 19 Upconverted fluorescence spectra (with progressively longer excitation wavelengths from 700 to 900 nm in 50 nm increments) of a kind of nitrogen-doped CDs. Produced with permission from ref. [108]

fluorescence and red-shift the luminescene of X-CDs wih a high QY of 16.5% by simply adding H_2O_2 in a hydrothermal process. This upconverted fluorescence property was also assigned to a multiphoton active process [127]. Gong's group has first focused on the two-photon fluorescence property of X-CDs and the research about their application as two-photon fluorescent probe for deep tissue imaging. They think that the large π-conjugated system in nitrogen-doped CDs and strong electron donating effect of dimethylamide improve the charge transfer efficiency to impart strong two-photon-induced fluorescence [64]. Jiang et al. prepared a kind of heteroaom-doped CDs which show UC properties not only in solutions but also in polymer films with a femtosecond pulse laser [50]. In Ananthanarayanan's opinion, the co-existence of electron donating and withdrawing sites which can come into being p-n type photochemical diodes in X-CDs results to its strong two-photon UC properties [93].

Fluorescent mechanisms

Currently, many groups have presented various mechanisms to uncover the fluorescent origin of CD-s including X-CDs, which may guide tuning the performance of the X-CDs. In Pan's opinion, the fluorescence is attributed to the free zigzag sites with a carbine-like triplet ground stage [128]. Afterwards, Zhu et al. presented that the co-existence of defect state emission and intrinsic state emission and their competitive emission centers lead to green and blue emission, explaining most of the fluorescent features [129]. Another assumption made by Liu et al. thought that the π-π electron transition contributes to the fluorescence and strong electron donating effect of functional groups can boost the charge transfer efficiency [64]. In addition, the size of CDs is also thought to be the possible reasons for the excitation-dependent phenomenon that fluorescent emissions can red-shift as the increase of the excitation wavelength [25]. Nevertheless, the fluorescent mechanism of CDs is still not completely understood, and the CDs synthesized via different methods may process fluorescence of different origin as well as the heterogeneity of CDs particles from the same synthesis.

Bioimaging

As fluorescent nanomaterials with bright fluorescence, high QY, resistance to photobleaching, biocompatibility and low biotoxicity, X-CDs are superior to current organic and inorganic fluorophores dueto the unique combination of a number of vital merits and show great potential for fluorescent bioimaging. X-CDs are attractive in the biomedical field as an imaging and labeling to track molecular targets in live cells, tissue or other biosystems [23, 25].

Cells imaging

X-CDs are readily taken by cells, in which fluorescence imaging can proceed with both one- and multiple-photon excitations [81, 93, 120, 130–132]. Ke et al. prepared nitrogen-doped CDs with emission in the visible region for HeLa cell imaging [122]. Upon incubation for 1.5 h with the CDs and then with Hoechst34580 (a dye to stain nuclei), the merged image proves the different localiziaon between the two labels, indicating that the nitrogen-doped CDs can penetrate into the cells and maintain their fluorescent properties in the cellular environment (Fig. 20). Yang et al. used selenium-doped CDs for fluorescence sensing of OH• in living cells. The selenium-doped CDs emitted orange fluorescence around their nuclei (Fig. 21b), while the introduction of OH• led to fluorescence quenching (Fig. 21d). Moreover, the added GSH was able to recover the fluorescence (Fig. 21f), confirming that the selenium-doped CDs were capable of sensing redox cycles in living cells [76]. A type of X-CDs conjugated with insulin were utilized for dynamic tracking of insulin receptors in adipocytes by Chen's group who investigated the dynamic trafficking of insulin receptors by total internal reflection fluorescence microscopy (TIRFM) [133]. Time-lapse images demonstrated that these X-CDs can be used to specifically track molecular targets involved in dynamic cellular process (Fig. 22).

Tissue imaging

In addition to cellular imaging, X-CDs can also be widely used for in vivo bioimaging. Yang et al. reported the study of nitorgen-doped CDs for fluorescent tissues imaging (Fig. 23) [134]. The nitrogen-doped CDs solution was intravenously injected into mice for whole-body circulation, then only emissions from the bladder area were observed. After 3 h postinjection, bright fluorescence was visible in the urine. At 4 h, only the kidney and liver among the organs showed detectable fluorescence, consistent with the urine excretion pathway.

Chen's group has doped CDs by conjugating the fluorescence dye ZW800 to the CDs to extend the spectra range to red (Fig. 24) [135]. The red fluorescent CDs were tracked in vivo for their biodistribution and excretion. The X-CDs were most rapidly excreted from the body after injection in intravenous route. The CDs were dominantly trapped in kidneys. It took only one hour to post intravenous injection. In their study, heteroatom-

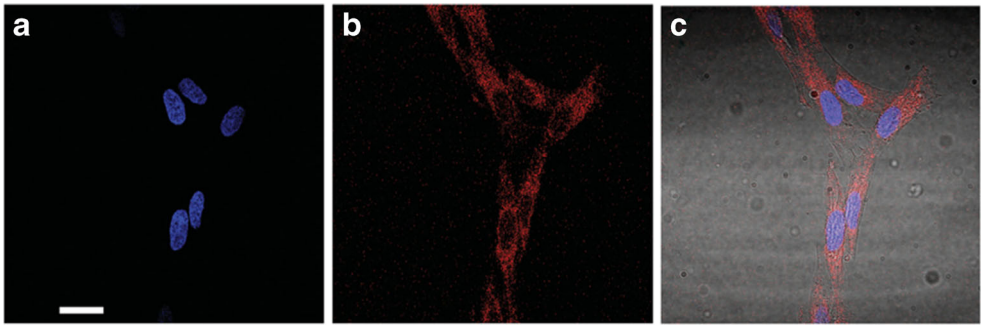

Fig. 20 Confocal microscopy images of HeLa cells laveled with (A) Hoechst 34,580 and (B) nitrogen-doped CDs. (C) The overlay of panels (**a**) and (**b**). The scale bar is 30 μm. Produced with permission from ref. [122]

doped CDs exhibited great potential as a nanoplatform for preclinical biomedical research for imaging-guided surgery.

Ge et al. developed a kind of sulfur-doped CDs with red emission as multimodal fluorescent, photoacoustic and thermal theranostics [71]. In the fluorescent imaging part, they

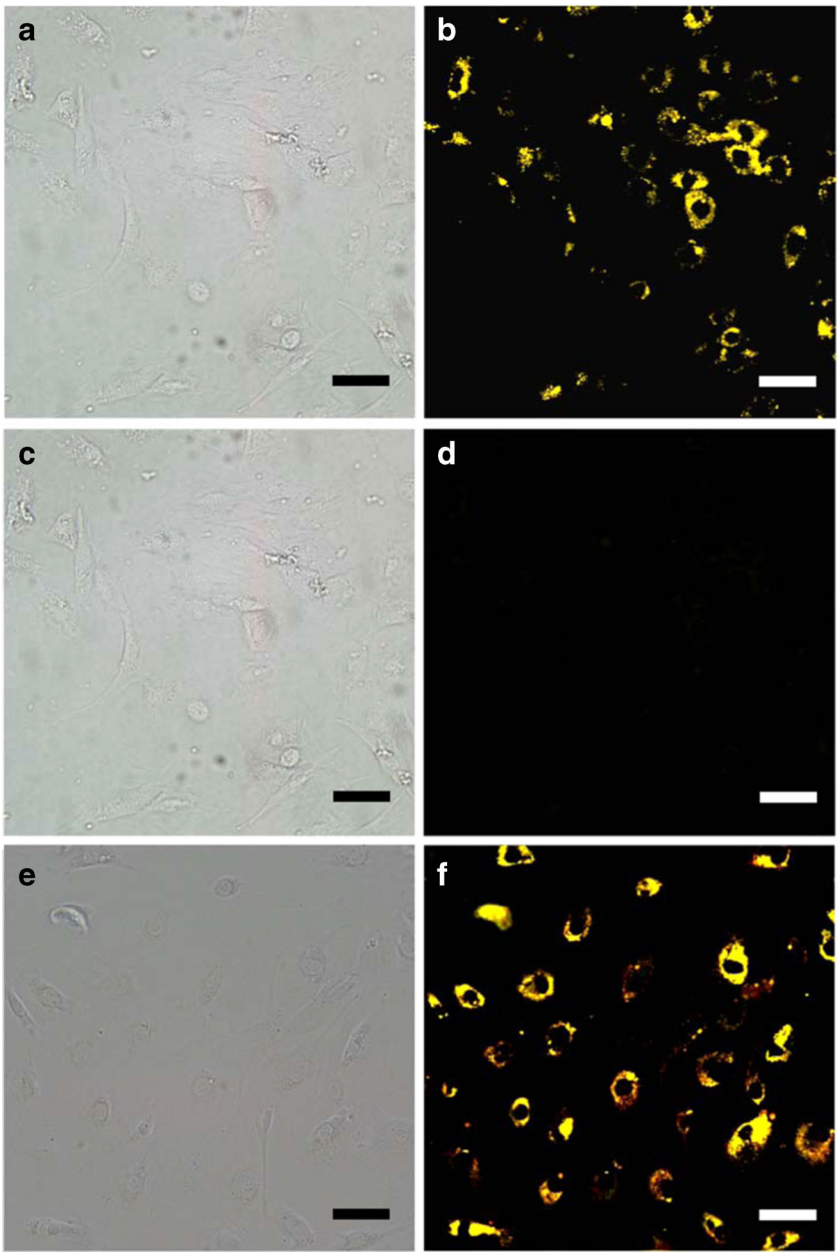

Fig. 21 Practical applications of switch system in vivo. HeLa cells loaded with selenium-doped CDs. **a** Brightfield image of selenium-doped CDs-loaded cells, **b** corresponding confocal fluorescence microphotograph of **a**. **c** Bright-field image of Se-GQD-loaded cells treated with H_2O_2 and M $FeSO_4$ for 10 min. **d** Corresponding confocal fluorescence microphotograph of **c**. **e** Bright-field image of selenium-doped CDs loaded cells exposed to a dose of GSH for an additional 10 min. **f** Corresponding confocal fluorescence microphotograph of **e**. Scale bar: 20 μm. Produced with permission from ref. [76]

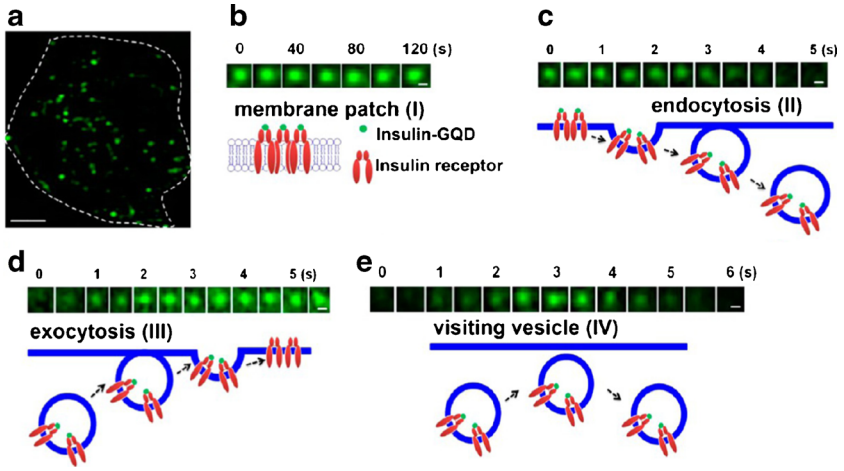

Fig. 22 Tracking the dynamics of insulin receptors in living adipocytes using TIRFM. **a** Typical TIRFM image of a 3 T3-L1adipocyte after 1 h incubation of insulin-GQDs. Scale bar =5 μm. **b** Membrane patch consisting of insulin-GQD/insulin receptor clusters (type I). **c** Endocytosis of fluorescent membrane patches into a vesicle (type II). **d** Exocytosis of a vesicle containing insulin-GQD/insulin receptor complexes (type III). **e** Transient approaching and retrieval of insulin-GQD/insulin receptor containing vesicle (type IV). Scale bars =0.2 μm. Produced with permission from ref. [133]

selected HeLa tumor-bearing nude mice as the animal model. As shown in Fig. 25, after injection, the sulfur-doped CDs accumulated in the tumor area by means of the enhanced permeability and retention effect and significant fluorescence was detected in the tumor area. After being sacrificed, the major organs (heart, liver, spleen, lung, and kidneys) of the mice were excised and imaged to evaluate the fluorescence intensities (Fig. 25b). The tumor tissue showed high fluorescence intensity, while the spleen and heart had little signals. The sulfur-doped CDs mainly distributed in the lung, liver and kidney tissues (Fig. 25c).

For in vivo bioimaging applications, the information on the maximum tissue penetration depth of heteroatom-doped CDs is required and Liu et al. investigated the imaging depth in turbid tissue phantom to explore the potential use of the strongly fluorescent nitrogen-doped CDs for the first time [64]. As shown in the schematic of the setup (Fig. 26a), a gap with adjustable height was built between both ends of the two coverslips. In the tunable gap was a solution of intralipid. Nitrogen-doped CDs were dripped and dried on the top coverslip. An inverted two-photon microscope was used to image the nitrogen-

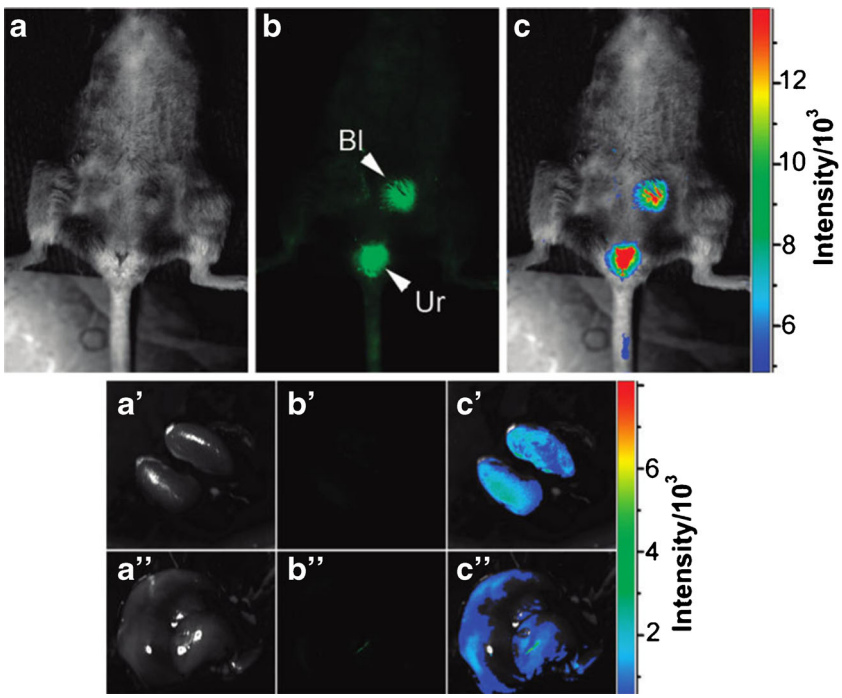

Fig. 23 A nitrogen-doped CDs dot solution was intravenously injected into mice for whole body circulation. **a** Bright field, **b** detected fluorescence (Bl: bladder and Ur: urine) and **c** color-coded images. The same order for the images of the dissected kidneys (a' – c') and liver (a" – c"lower right). Produced with permission from ref. [134]

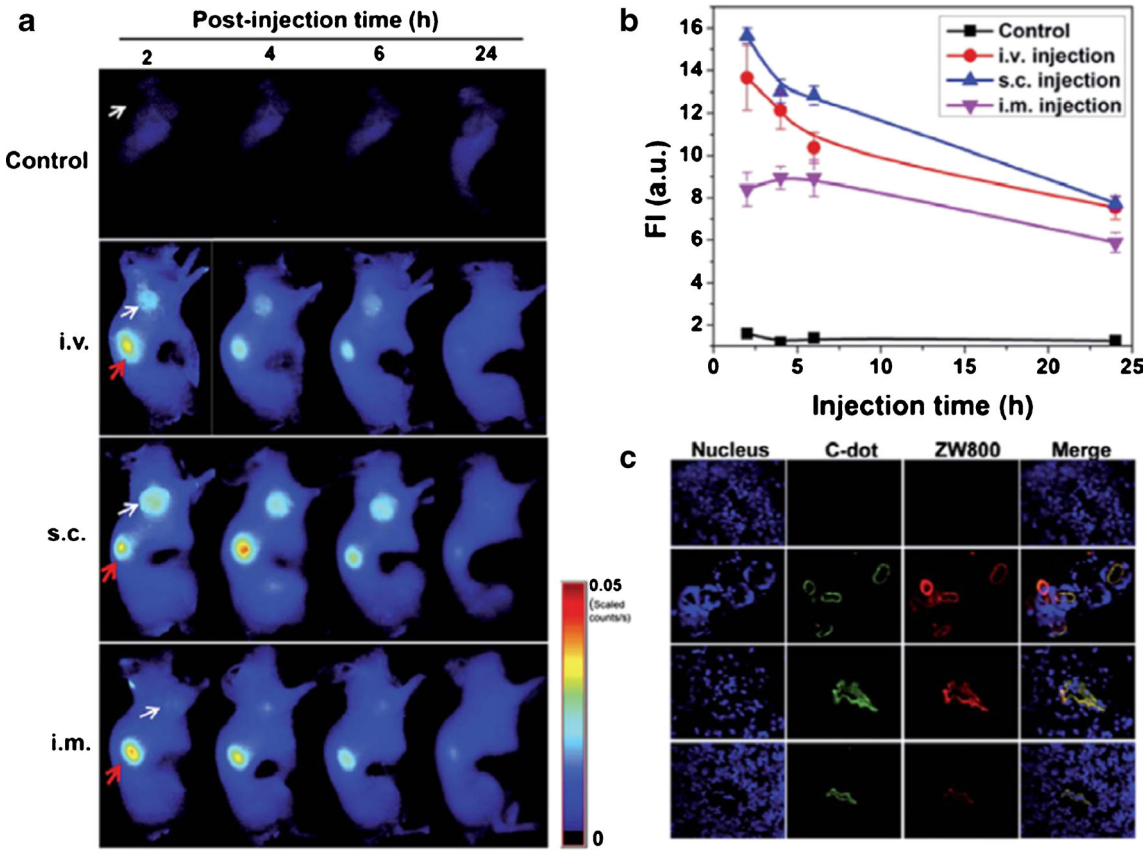

Fig. 24 Tumor uptake of ZW800–carbon dots after different routes of injection. **a** NIR fluorescence images of SCC-7 tumor-bearing mice acquired at 2, 4, 6, and 24 h post-injection: control (without injection); iv injection; sc injection; im injection (white arrow indicates tumor; red arrow indicates kidney). **b** Tumor region of interest nalysis. Fluorescence signal unit: $\times 10^8$ photons per cm^2 per s^1. **c** Ex vivo fluorescence images derived from the emission of carbon dots and ZW800 were acquired to confirm tumor uptake of particles. Produced with permission from ref. [135]

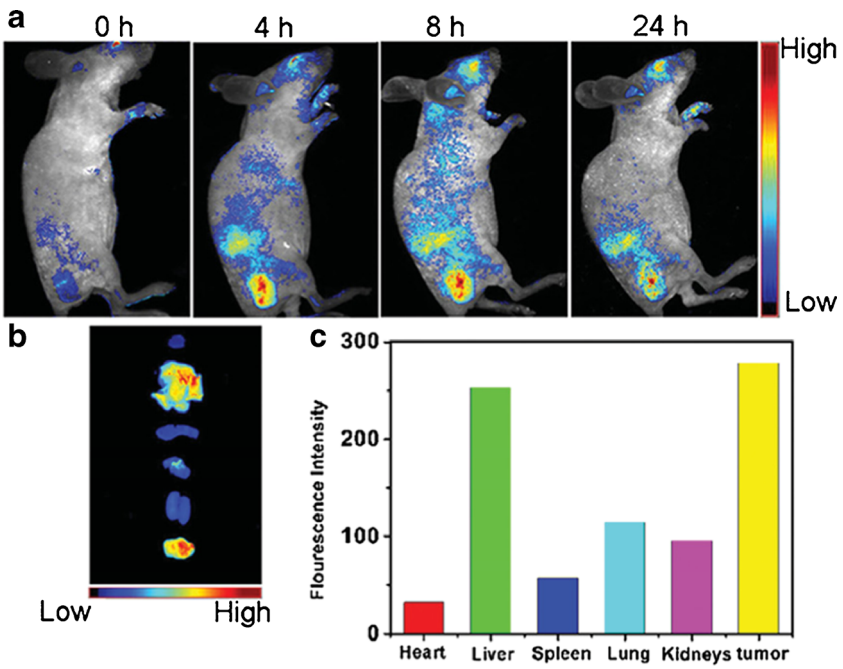

Fig. 25 In vivo fluorescent imaging. **a** Real-time in vivo red fluorescent images after i.v. injection of CDs in nude mice at different time points. **b** Ex vivo images of mice tissues (from top to bottom: heart, liver, spleen, lung, kidneys, tumor). **c** Average fluorescent intensities from the tumor area at 24 h postinjection ($n = 5$). Produced with permission from ref. [71]

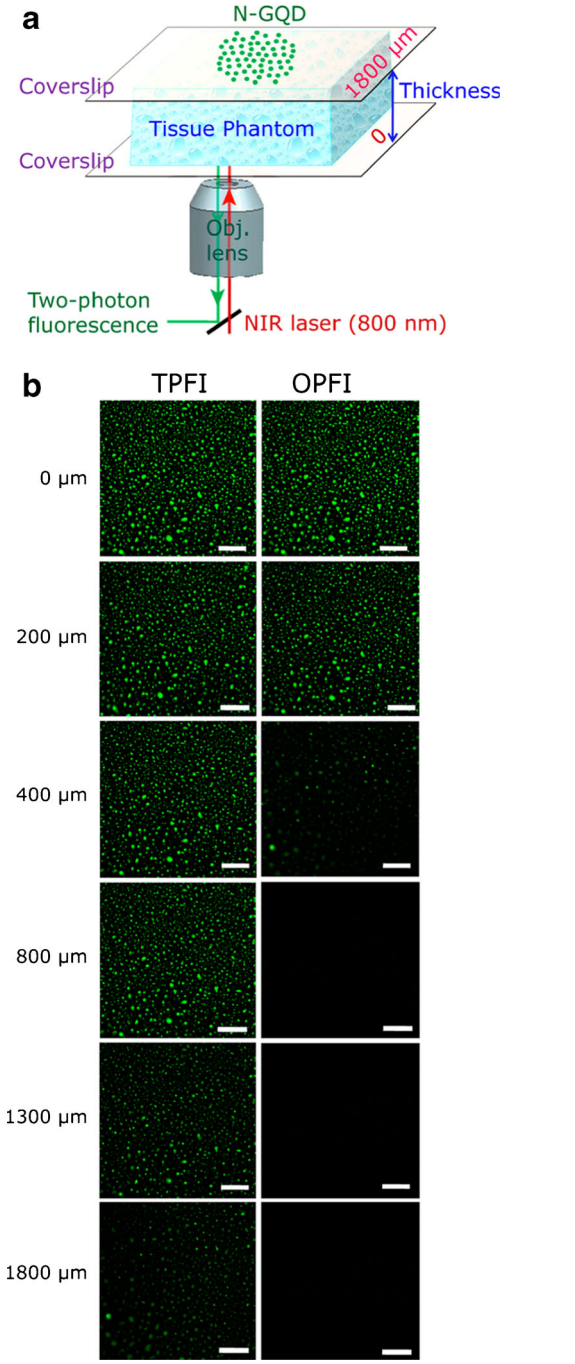

Fig. 26 **a** Schematic of the setup used for two-photon fluorescence imaging of nitrogen-doped CDs in tissue phantom with different thickness. **b** Penetration depth of nitrogen-doped CDs for two-photon fluorescence imaging (left panel) and one-photon fluorescence imaging (right panel) in tissue phantom (all scale bar: 100 μm). Produced with permission from ref. [64]

doped CDs at different depths in the mock tissue. The resulting images (Fig. 26) indicated that the nitrogen-doped CDs can be imaged at depths ranging from 0 to 1800 μm with high signal-to-noise ratio, which was far exceeding that of the organic dyes and suitable for in vivo bioimaging applications.

Others

Besides above mentioned, fluorescent probes are widely used in imaging of many other biological samples, which include more than zebrafish [136], *Arabidopsis thaliana* [137], *Staphylococcus aureus* [138], *Escherichia coli* [139] and *C. elegans* [140]. Heterotaoms-doped CDs have been coming into prominence as fluorescent probes in biological samples like these. Saxena et al. parpared a kind of X-CDs and used them to image the full life cycle of mosquitoes (Fig. 27) [138]. Interestingly, the X-CDs not only can image the mosquitoes in different stages but also suggest that hetroatoms-doped CDs retard the hormonal activity to slow down the larval growth with progressive delay in moulting. Further fluorescent imaging on mout at early stages proved that X-CDs were gradually released from the body in the ecdysis and these fluorescent mosquitos excreted out the fluorescent stuff present in theier body upon relocaton of CDs treated mosquitoes half way into the fresh water. Zhai et al. presented an ingenious

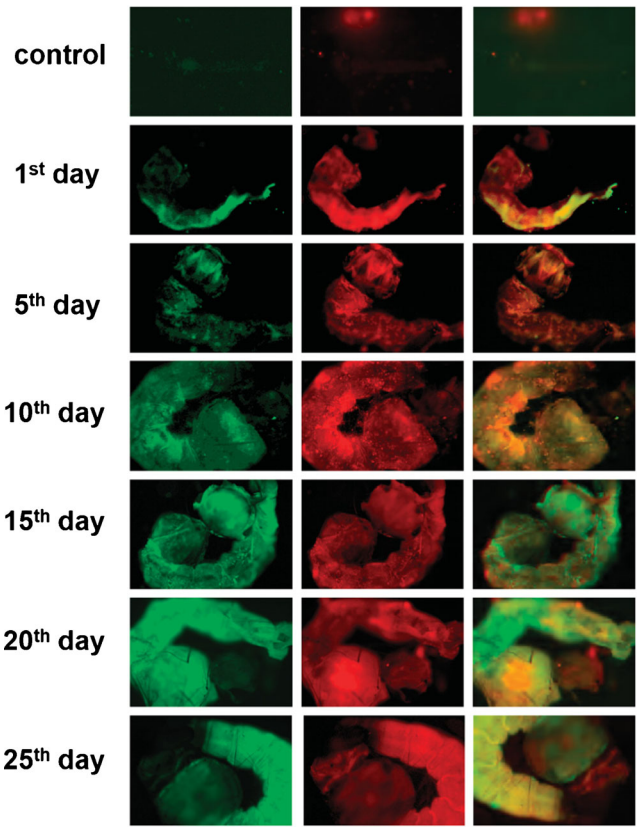

Fig. 27 Growing larvae of mosquito treated with X-CDs. The 1 st row represents the auto fluorescence of the control mosquito larvae. The remaining six rows (from top to bottom) represent fluorescence images on various days (1–25) for treated larvae of mosquito. Left, middle and right column images are those observed under 488 nm, 561 nm and the merged image of 488/561 nm band pass filters, respectively. Produced with permission from ref. [141]

method for the fabrication of nitrogen-doped CDs, which are a super fluorescent bioimaging agent in urine, bean sprouts and mice [141].

Summary and future perspective

In this review, X-CDs have been comprehensively introduced from the aspect of design strategies, doping species, properties, some PL mechanisim and applications for bioimaging. In addition, the heteroaoms-doped CDs are potential materials for both in vitro and in vivo bioimaging. The use of X-CDs for bioimaging has achieved great success within a short time. UC and IR fluorescent X-CDs for live deep-tissue imaging and for targeted cancer imaging, diagnosis and therapy are particularly desired. Herein, we speculate the future perspectives on bioimaging of X-CDs.

(1) Exploit X-CDs with excellent performance of red/near-IR/UC emission, high QY, ready aqueous solubility, easy surface functionalization and low cytotoxicity simultaneously to meet the multifunctional application demand for both *invivo* bioimaging and *invitro* assay detection, thus more effective in tissue penetration, is desired. Current CDs based probes still have some drawbacks more or less in some aspects and are far from more practical requirements. For instance, the emissions of CDs can go to longer by further increasing the excitation wavelength, while the intensity is usually rather low.

(2) Develop X-CDs for response modes such as luminescence turn-on, FRET, and ratio metric response. Most CDs based response is depended on the turn-off mode of fluorescence, which inclines to be interfered by the environmental factors. At present, the fluorescent imaging of trace levels of analyte is still difficult and thus the turn-off mode shows no obvious advantage owing to its high background signal. Yet, other response modes have the advantage of high detecton sensitivity or eliminating the interering influences from many factors.

(3) Design fluorescence lifetime imaging of X-CDs to offload the interference of auto-fluorescence of biological amples and avoid the effect of the experiment conditions on the fluorescence intensity, making the sensitive and accurate measuement of analytes in biosystms possible. To our knowledge, there have been rare reports of CDs in this area. This potential property required to be exploited in the near future.

(4) Synthesize CDs based nanotructures composed of multiple targeting, imaging and therapeutic modules. For instance, the integrating with magnetic resonance imaing (MRI) contrast agents or radionudides may providing platform for dual-mode imaging, while X-CDs with modular surface chemistry can serve as traceable delivery vehicles and bioimaging agents when combind with nucleic acid therapeutics. The exploitation of functional X-CDs for controlled coupling with bioactive species would help to design of a multifunctional platform with specific cell type targeting, diagnosis and therapy applications, and further investigations are needed in particular for X-CDs.

(5) Study the detailed machanism fo PL in X-CDs. Although some possoble mechanisms have been presented, such as size effect, charge transfer, molecul-like states, and the competition between the intrinsic state and the defect state emissions, they are various and not unified. The fluorescence mechanism of CDs including X-CDs is still not solved completely, so the combination of more theoretical and experimental works is urgently expected. Researchers should take advantage of sufficient characterization methods to elucidate the PL mechanism. Their accurate mechanism of cellular uptake and toxicological effect needs to be illuminated.

As present above, X-CDs, as a new nanomaterial, have inspired intensive research and provided unprecedented possibilities in bioimaging although this area is still in its infant stage. Hopefully, this article would stimulage continued interest and endeavors in the fluorescent bioimaging area of X-CDs.

Acknowledgments This project was supported by grants from National Natural Science Foundation of China (81274093), Shandong Province Natural Science Foundation (ZR2015HL128), Health Department of Shandong province (2014WS0478). We thank coworkers for help and constructive suggestions.

Compliance with ethical standards The author(s) declare that they have no competing interests.

References

1. Zhu SJ, Meng QN, Wang L, Zhang JH, Song YB, Jin H, Zhang K, Sun HC, Wang HY, Yang B (2013) Highly photoluminescent carbon dots for multicolor patterning, sensors, and bioimaging. Angew Chem 52(14):3953–3957
2. Wang GY, Shi GF, Chen XF, Yao RX, Chen FW (2015) A glassy carbon electrode modified with graphene quantum dots and silver nanoparticles for simultaneous determination of guanine and adenine. Microchim Acta 182(1):315–322
3. Bhaisare ML, Talib A, Khan MS, Pandey S, Wu HF (2015) Synthesis of fluorescent carbon dots via microwave carbonization of citric acid in presence of tetraoctylammonium ion, and their application to cellular bioimaging. Microchim Acta 182(13): 2173–2181
4. Wang B, Chen YF, Wu YY, Weng B, Liu YS, Li CM (2016) Synthesis of nitrogen- and iron-containing carbon dots, and their application to colorimetric and fluorometric determination of dopamine. Microchim Acta 183(9):2491–2500

5. Liu BB, Han SQ (2016) Determination of trace hydrogen sulfide by using the permanganate induced chemiluminescence of carbon dots. Microchim Acta. doi:10.1007/s00604-016-1957-6
6. Xu XY, Ray R, Gu YL, Ploehn HJ, Gearheart L, Raker K, Scrivens WA (2004) Electrophoretic analysis and purification of fluorescent single-walled carbon nanotube fragments. J Am Chem Soc 126(40):12736–12737
7. Song YB, Zhu SJ, Yang B (2014) Bioimaging based on fluorescent carbon dots. RSC Adv 4(52):27184–27200
8. Zhou J, Shan XY, Ma JJ, Gu YM, Qian ZS, Chen JR, Feng H (2014) Facile synthesis of P-doped carbon quantum dots with highly efficient photoluminescence. RSC Adv 4(11):5465–5468
9. Chen H, Wang ZY, Zong SF, Chen P, Zhu D, Wu L, Cui YP (2015) A graphene quantum dot-based FRET system for nuclear-targeted and real-time monitoring of drug delivery. Nanoscale 7(37): 15477–15486
10. Martindale BCM, Hutton GAM, Caputo CA, Reisner E (2015) Solar hydrogen production using carbon quantum dots and a molecular nickel catalyst. J Am Chem Soc 137(18):6018–6025
11. Guo CX, Yang HB, Sheng ZM, Lu ZS, Song QL, Li CM (2010) Layered graphene/quantum dots for photovoltaic devices. Angew Chem Int Ed 49(17):3014–3017
12. Ji LJ, Chen L, Wu P, Gervasio DF, Cai CX (2016) Highly selective fluorescence determination of the hematin level in human erythrocytes with no need for separation from bulk hemoglobin. Anal Chem 88(7):3935–3944
13. Li N, Than A, Wang XW, Xu SH, Sun L, Duan HW, Xu CJ, Chen P (2016) Ultrasensitive profiling of metabolites using tyramine-functionalized graphene quantum dots. ACS Nano 10(3):3622–3629
14. Wang YF, Hu AG (2014) Carbon quantum dots: synthesis, properties and applications. J Mater Chem C 2(34):6921–6939
15. Chen W, Liu CR, Peng B, Zhao Y, Pacheco A, Xian M (2013) New fluorescent probes for sulfane sulfurs and the application in bioimaging. Chem Sci 4(7):2892–2896
16. Chen W, Rosser EW, Matsunaga T, Pacheco A, Akaike T, Xian M (2015) The development of fluorescent probes for visualizing intracellular hydrogen polysulfides. Angew Chem Int Ed 54(47): 13961–13965
17. Chen W, Rosser EW, Zhang D, Shi W, Li YL, Dong WJ, Ma HM, Hu DH, Xian M (2015) A specific nucleophilic ring-opening reaction of aziridines as a unique platform for the construction of hydrogen polysulfides sensors. Org Lett 17(11):2776–2779
18. Chen W, Pacheco A, Takano Y, Day JJ, Hanaoka K, Xian M (2016) A single fluorescent probe to visualize hydrogen sulfide and hydrogen polysulfides with different fluorescence signals. Angew Chem Int Ed 55(34):9993–9996
19. Zheng XT, Ananthanarayanan A, Luo KQ, Chen P (2015) Glowing graphene quantum dots and carbon dots: properties, syntheses, and biological applications. Small 11(14):1620–1636
20. Zuo PL, Lu XH, Sun ZG, Guo YH, He H (2016) A review on syntheses, properties, characterization and bioanalytical applications of fluorescent carbon dots. Microchim Acta 183(2):519–542
21. Fan ZT, Li SH, Yuan FL, Fan LZ (2015) Fluorescent graphene quantum dots for biosensing and bioimaging. RSC Adv 5(25): 19773–19789
22. Du Y, Guo SJ (2016) Chemically doped fluorescent carbon and graphene quantum dots for bioimaging, sensor, catalytic and photoelectronic applications. Nanoscale 8(5):2532–2543
23. Wang AJ, Li H, Huang H, Qian ZS, Feng JJ (2016) Fluorescent graphene-like carbon nitrides: synthesis, properties and applications. J Mater Chem C 4(35):8146–8160
24. Zhu SJ, Song YB, Zhao XH, Shao JR, Zhang JH, Yang B (2015) The photoluminescence mechanism in carbon dots (graphene quantum dots, carbon nanodots, and polymer dots): current state and future perspective. Nano Res 8(2):355–381
25. Wang ZF, Zeng HD, Sun LY (2015) Graphene quantum dots: versatile photoluminescence for energy, biomedical, and environmental applications. J Mater Chem C 3(6):1157–1165
26. Lin LP, Rong MC, Luo F, Chen D, Wang YR, Chen X (2014) Luminescent graphene quantum dots as new fluorescent materials for environmental and biological applications. Trends Anal Chem 54:83–102
27. Luo PG, Yang F, Yang ST, Sonkar SK, Yang LJ, Broglie JJ, Liu Y, Sun YP (2014) Carbon-based quantum dots for fluorescence imaging of cells and tissues. RSC Adv 4(21):10791–10807
28. Wolfbeis OS (2015) An overview of nanoparticles commonly used in fluorescent bioimaging. Chem Soc Rev 44(14):4743–4768
29. Wang QL, Zheng HZ, Long YJ, Zhang LY, Gao M, Bai WJ (2011) Microwave–hydrothermal synthesis of fluorescent carbon dots from graphite oxide. Carbon 49(9):3134–3140
30. Tao H, Yang K, Ma Z, Wan J, Zhang Y, Kang Z, Liu Z (2012) In vivo NIR fluorescence imaging, biodistribution, and toxicology of photoluminescent carbon dots produced from carbon nanotubes and graphite. Small 8(2):281–290
31. Peng J, Gao W, Gupta BK, Liu Z, Romero-Aburto R, Ge L, Song L, Alemany LB, Zhan X, Gao G, Vithayathil SA, Kaipparettu BA, Marti AA, Hayashi T, Zhu JJ, Ajayan PM (2012) Graphene quantum dots derived from carbon fibers. Nano Lett 12(2):844–849
32. Dong YQ, Chen CQ, Zheng XT, Gao LL, Cui ZM, Yang HB, Guo CX, Chi YW, Li CM (2012) One-step and high yield simultaneous preparation of single- and multi-layergraphene quantum dots from CX-72 carbon black. J Mater Chem 22(18):8764–8766
33. Qiao ZA, Wang YF, Gao Y, Li HW, Dai TY, Liu YL, Huo QS (2010) Commercially activated carbon as the source for producing multicolor photoluminescent carbon dots by chemical oxidation. Chem Commun 46(46):8812–8814
34. Qian ZS, Zhou J, Chen JR, Wang C, Chen CC, Feng H (2011) Nanosized N-doped graphene oxide with visible fluorescence in water for metal ion sensing. J Mater Chem 21(44):17635–17637
35. Rong MC, Song XH, Zhao TT, Yao QH, Wang YR, Chen X (2015) Synthesis of highly fluorescent P,O-g-C_3N_4 nanodots for the label-free synthesis of highly fluorescent P,O-g-C_3N_4 nanodots for the label-free detection of Cu^{2+} and acetylcholinesterase activity. J Mater Chem C 3(41):10916–10924
36. Zhu SJ, Zhang JH, Qiao CY, Tang SJ, Li YF, Yuan WJ, Li B, Tian L, Liu F, Hu R, Gao HN, Wei HT, Zhang H, Sun HC, Yang B (2011) Strongly green-photoluminescent graphene quantum dots for bioimaging applications. Chem Commun 47(24):6858–6860
37. Hu CF, Liu YL, Yang YH, Cui JH, Huang ZR, Wang YL, Yang LF, Wang HB, Xiao Y, Rong JH (2013) One-step preparation of nitrogen-doped graphene quantum dots from oxidized debris of graphene oxide. J Mater Chem B 1(1):39–42
38. Lu J, Yang JX, Wang JZ, Lim AL, Wang SA, Loh KP (2009) One-pot synthesis of fluorescent carbon nanoribbons, nanoparticles, and graphene by the exfoliation of graphite in ionic liquids. ACS Nano 3(8):2367–2375
39. Li Y, Zhao Y, Cheng HH, Hu Y, Shi GQ, Dai LM, Qu LT (2012) Nitrogen-doped graphene quantum dots with oxygen-rich functional groups. J Am Chem Soc 134(1):15–18
40. Ananthanarayanan A, Wang X, Routh P, Sana B, Lim S, Kim DH, Lim KH, Li J, Chen P (2014) Facile synthesis of graphene quantum dots from 3D graphene and their application for Fe^{3+} sensing. Adv Funct Mater 24(20):3021–3026
41. Fan ZT, Li YC, Li XH, Fan LZ, Zhou SX, Fang DC, Yang SH (2014) Surrounding media sensitive photoluminescence of boron-doped graphene quantum dots for highly fluorescent dyed crystals, chemical sensing and bioimaging. Carbon 70:149–156
42. Li SH, Li YC, Cao J, Zhu J, Fan LZ, Li XH (2014) Sulfur-doped graphene quantum dots as a novel fluorescent probe for highly

selective and sensitive detection of Fe^{3+}. Anal Chem 86(20): 10201–10207
43. Sun YP, Zhou B, Lin Y, Wang WJ, Fernando KAS, Pathak P, Meziani MJ, Harruff BA, Wang X, Wang H, Luo PJG, Yang H, Kose ME, Chen B, Veca LM, Xie SY (2006) Quantum-sized carbon dots for bright and colorful colorful photoluminescence. J Am Chem Soc 128(24):7756–7757
44. Li LL, Ji J, Fei R, Wang CZ, Lu Q, Zhang JR, Jiang LP, Zhu JJ (2012) A facile microwave avenue to electrochemiluminescent two-color graphene quantum dots. Adv Funct Mater 22(14): 2971–2979
45. Zhuo SJ, Shao MW, Lee ST (2012) Upconversion and downconversion fluorescent graphene quantum dots: ultrasonic preparation and photocatalysis. ACS Nano 6(2):1059–1064
46. Tian J, Liu Q, Asiri AM, Al-Youbi AO, Sun X (2013) Ultrathin graphitic carbon nitride nanosheet: a highly efficient fluorosensor for rapid, ultrasensitive detection of Cu^{2+}. Anal Chem 85(11): 5595–5599
47. Wang WP, Lu YC, Huang H, Feng JJ, Chen JR, Wang AJ (2014) Facile synthesis of water-soluble and biocompatible fluorescent nitrogen-doped carbon dots for cell imaging. Analyst 139(7): 1692–1696
48. Pan LL, Sun S, Zhang AD, Jiang K, Zhang L, Dong CQ, Huang Q, Wu AG, Lin HW (2015) Truly fluorescent excitation-dependent carbon dots and their applications in multicolor cellular imaging and multidimensional sensing. Adv Mater 27(47):7782–7787
49. Jiang K, Sun S, Zhang L, Lu Y, Wu AG, Cai CZ, Lin HW (2015) Red, green, and blue luminescence by carbon dots: full-color emission tuning and multicolor cellular imaging. Angew Chem Int Ed 54(18):5360–5363
50. Guan WW, Gu W, Ye L, Guo CY, Su S, Xu PX, Xue M (2014) Microwave-assisted polyol synthesis of carbon nitride dots from folic acid for cell imaging. Int J Nanomedicine 9:5071–5078
51. Wang W, Li YM, Cheng L, Cao ZQ, Liu WG (2014) Watersoluble and phosphorus-containing carbon dots with strong green fluorescence for cell labeling. J Mater Chem B 2(1):46–48
52. Li H, Shao FQ, Huang H, Feng JJ, Wang AJ (2016) Eco-friendly and rapid microwave synthesis of green fluorescent graphitic carbon nitride quantum dots for vitro bioimaging. Sensors Actuators B Chem 226:506–511
53. Liao B, Long P, He BQ, Yi SJ, Ou BL, Shen SH, Chen J (2013) Reversible fluorescence modulation of spiropyran-functionalized carbon nanoparticles. J Mater Chem C 1(23):3716–3721
54. Zheng M, Liu S, Li J, Qu D, Zhao HF, Guan XG, Hu XL, Xie ZG, Jing XB, Sun ZC (2014) Integrating oxaliplatin with highly luminescent carbon dots: an unprecedented theranostic agent for personalized medicine. Adv Mater 26(21):3554–3560
55. Wang J, Zhang ZH, Zha S, Zhu YY, Wu PY, Ehrenberg B, Chen JY (2014) Carbon nanodots featuring efficient FRET for two-photon photodynamic cancer therapy with a low fs laser power density. Biomaterials 35(34):9372–9381
56. Liu XJ, Zhang N, Bing T, Shangguan DH (2014) Carbon dots based dual-emission silica nanoparticles as a ratiometric nanosensor for Cu^{2+}. Anal Chem 86(5):2289–2296
57. Jiang F, Chen DQ, Li RM, Wang YC, Zhang GQ, Li SM, Zheng JP, Huang NY, Gu Y, Wang CR, Shu CY (2013) Eco-friendly synthesis of size-controllable aminefunctionalized graphene quantum dots with antimycoplasma properties. Nanoscale 5(3):1137–1142
58. Dong YQ, Wang RX, Li H, Shao JW, Chi YW, Lin XM, Chen GN (2012) Polyamine-functionalized carbon quantum dots for chemical sensing. Carbon 50(8):2810–2815
59. Sk MA, Ananthanarayanan A, Huang L, Lim KH, Chen P (2014) Revealing the tunable photoluminescence properties of graphene quantum dots. J Mater Chem C 2(34):6954–6960
60 Qian ZS, Zhou J, Ma JJ, Shan XY, Chen CC, Chen JR, Feng H (2013) The visible photoluminescence mechanism of oxidized multi-walled carbon nanotubes: an experimental and theoretical investigation. J Mater Chem C 1(2):307–314
61 Choi Y, Kim S, Choi MH, Ryoo SR, Park J, Min DH, Kim BS (2014) Highly biocompatible carbon nanodots for simultaneous bioimaging and targeted photodynamic therapy in vitro and in vivo. Adv Funct Mater 24(37):5781–5789
62 Shao TL, Wang GD, An XT, Zhuo SJ, Xia YS, Zhu CQ (2014) A reformative oxidation strategy using high concentration nitric acid for enhancing the emission performance of graphene quantum dots. RSC Adv 4(89):47977–47981
63 Liu Q, Guo B, Rao Z, Zhang B, Gong JR (2013) Strong two-photon-induced fluorescence from photostable, biocompatible nitrogen-doped graphene quantum dots for cellular and deep-tissue imaging. Nano Lett 13(6):2436–2441
64 Wang L, Wang YL, Xu T, Liao HB, Yao CJ, Liu Y, Li Z, Chen ZW, Pan DY, Sun LT, Wu MH (2014) Gram-scale synthesis of single-crystalline graphene quantum dots with superior optical properties. Nat Commun 5:5357–5365
65 Sternschulte H, Thonke K, Sauer R, Koizumi S (1999) Optical evidence for 630-meV phosphorus donor in synthetic diamond. Phys Rev B: Condens Matter Mater Phys 59(20):12924–12927
66 Sarkar S, Das K, Ghosh M, Das PK (2015) Amino acid functionalized blue and phosphorousdoped green fluorescent carbon dots as bioimaging probe. RSC Adv 5(81):65913–65921
67 Macdonald F, Lide DR (2003) CRC handbook of chemistry and physics, 84th edn. CRC Press, Boca Raton
68 Gao H, Liu Z, Song L, Guo W, Gao W, Ci L, Rao A, Quan W, Vajtai R, Ajayan PM (2012) Synthesis of S-doped graphene by liquid precursor. Nanotechnology 23:275605
69 Chandra S, Patra P, Pathan SH, Roy S, Mitra S, Layek A, Bhar R, Pramanik P, Goswami A (2013) Luminescent S-doped carbon dots: an emergent architecture for multimodal applications. J Mater Chem B 1(18):2375–2382
70 Ge JC, Jia QY, Liu WM, Guo L, Liu QY, Lan MH, Zhang HY, Meng XM, Wang PF (2015) Red-emissive carbon dots for fluorescent, photoacoustic, and thermal theranostics in living mice. Adv Mater 27(28):4169–4177
71 Park CH, Yang H, Lee J, Cho HH, Kim D, Lee DC, Kim BJ (2015) Multicolor emitting block copolymer-integrated graphene quantum dots for dolorimetric, simultaneous sensing of temperature, pH, and metal ions. Chem Mater 27(15):5288–5294
72 Yu FB, Li P, Li GY, Zhao GJ, Chu TS, Han KL (2011) A near-IR reversible fluorescent probe modulated by selenium for monitoring peroxynitrite and imaging in living cells. J Am Chem Soc 133(29): 11030–11033
73 Xu KH, Qiang MM, Gao W, Su RX, Li N, Gao Y, Xie YX, Kong FP, Tang B (2013) A near-infrared reversible fluorescent probe for real-time imaging of redox status changes in vivo. Chem Sci 4(3): 1079–1086
74 Zhang W, Liu W, Li P, Kang JQ, Wang JY, Wang H, Tang B (2015) Reversible two-photon fluorescent probe for imaging of hypochlorous acid in live cells and in vivo. Chem Commun 51(50):10150–10153
75 Yang SW, Sun J, He P, Deng XX, Wang ZY, Hu CY, Ding GQ, Xie XM (2015) Selenium doped graphene quantum dots as an ultrasensitive redox fluorescent switch. Chem Mater 27(6):2004–2011
76 Qian ZS, Shan XY, Chai LJ, Ma JJ, Chen JR, Feng H (2014) Si-doped carbon quantum dots: a facile and general preparation strategy, bioimaging application, and multifunctional sensor. ACS Appl Mater Interfaces 6(9):6797–6805
77 Wang F, Xie Z, Zhang H, Liu CY, Zhang YG (2011) Highly luminescent organosilane-functionalized carbon dots. Adv Funct Mater 21(6):1027–1031

78 Tang Q, Zhou Z, Chen ZF (2013) Graphene-related nanomaterials: tuning properties by functionalization. Nanoscale 5(11):4541–4583

79 Zhang L, Zhang ZY, Liang RP, Li YH, Qiu JD (2014) Boron-doped graphene quantum dots for selective glucose sensing based on the "abnormal" aggregation-induced photoluminescence enhancement. Anal Chem 86(9):4423–4430

80 Hai X, Mao QX, Wang WJ, Wang XF, Chen XW, Wang JH (2015) An acid-free microwave approach to prepare highly luminescent boron-doped graphene quantum dots for cell imaging. J Mater Chem B 3(47):9109–9114

81 Shan XY, Chai LJ, Ma JJ, Qian ZS, Chen JR, Feng H (2014) B-doped carbon quantum dots as a sensitive fluorescence probe for hydrogen peroxide and glucose detection. Analyst 139(10):2322–2325

82 Bourlinos AB, Trivizas G, Karakassides MA, Baikousi M, Kouloumpis A, Gournis D, Bakandritsos A, Hola K, Kozak O, Zboril R, Papagiannouli I, Aloukos P, Couris S (2015) Green and simple route toward boron doped carbon dots with significantly enhanced non-linear optical properties. Carbon 83:173–179

83 Tasis D, Tagmatarchis N, Bianco A, Prato M (2006) Chemistry of carbon nanotubes. Chem Rev 106(3):1105–1136

84 Johns JE, Hersam MC (2013) Atomic covalent functionalizaiton of graphene. Acc Chem Res 46(1):77–86

85 Zhou J, Lin P, Ma JJ, Shan XY, Feng H, Chen CC, Chen JR, Qian ZS (2013) Facile synthesis of halogenated carbon quantum dots as an important intermediate for surface modification. RSC Adv 3(25):9625–9628

86 Sun HJ, Ji HW, Ju EG, Guan YJ, Ren JS, Qu XG (2015) Synthesis of fluorinated and nonfluorinated graphene quantum dots through a new top-down strategy for long-time cellular imaging. Chem Eur J 21(9):3791–3797

87 Qu D, Zheng M, Du P, Zhou Y, Zhang LG, Li D, Tan HQ, Zhao Z, Xie ZG, Sun ZC (2013) Highly luminescent S, N co-doped graphene quantum dots with broad visible absorption bands for visible light photocatalysts. Nanoscale 5(24):12272–12277

88 Lu YC, Chen J, Wang AJ, Bao N, Feng JJ, Wang WP, Shao LX (2015) Facile synthesis of oxygen and sulfur co-doped graphitic carbon nitride fluorescent quantum dots and their application for mercury (II) detection and bioimaging. J Mater Chem C 3(1):73–78

89 Huang H, Lu YC, Wang AJ, Liu JH, Chen JR, Feng JJ (2014) A facile, green, and solvent-free route to nitrogen-sulfur-codoped fluorescent carbon nanoparticles for cellular imaging. RSC Adv 4(23):11872–11875

90 Zhang BX, Gao H, Li XL (2014) Synthesis and optical properties of nitrogen and sulfur co-doped graphene quantum dots. New J Chem 38(9):4615–4621

91 Prasad KS, Pallela R, Kim DM, Shim YB (2013) Microwave-assisted one-pot synthesis of metal-free nitrogen and phosphorus dual-doped nanocarbon for electrocatalysis and cell imaging. Part Part Syst Charact 30(6):557–564

92 Ananthanarayanan A, Wang Y, Routh P, Sk MA, Than A, Lin M, Zhang J, Chen J, Sun HD, Chen P (2015) Nitrogen and phosphorus co-doped graphene quantum dots: synthesis from adenosine triphosphate, optical properties, and cellular imaging. Nanoscale 7(17):8159–8165

93 Liu SY, Zhao N, Cheng Z, Liu HG (2015) Amino-functionalized green fluorescent carbon dots as surface energy transfer biosensors for hyaluronidase. Nanoscale 7(15):6836–6842

94 Hou JY, Dong GJ, Tian ZB, Lu JT, Wang QQ, Ai SY, Wang ML (2016) A sensitive fluorescent sensor for selective determination of dichlorvos based on the recovered fluorescence of carbon dots-Cu(II) system. Food Chem 202(1):81–87

95 Qu D, Zheng M, Li J, Xie ZG, Sun ZC (2015) Tailoring color emissions from N-doped graphene quantum dots for bioimaging applications. Light Sci Appl 4:e364

96 Wu ML, Wang D, Wan LJ (2016) Directed block copolymer self-assembly implemented viasurface embedded electrets. Nat Commun 7:10752

97 Xu HB, Zhou SH, Xiao LL, Wang HH, Lia SZ, Yuan QH (2015) Fabrication of a nitrogen-doped graphene quantum dot from MOF-derived porous carbon and its application for highly selective fluorescence detection of Fe^{3+}. J Mater Chem C 3(2):291–297

98 Stan CS, Albu C, Coroaba A, Popa M, Sutiman D (2015) One step synthesis of fluorescent carbon dots through pyrolysis of N-hydroxysuccinimide. J Mater Chem C 3(4):789–795

99 Xue Q, Zhang HJ, Zhu MS, Wang ZF, Pei ZX, Huang Y, Huang Y, Song XF, Zeng HB, Zhi CY (2016) Hydrothermal synthesis of blue-fluorescent monolayer BN and BCNO quantum dots for bio-imaging probes. RSC Adv 6(82):79090–79094

100 Kavitha T, Kim JO, Jang S, Kim DP, Kang IK, Park SY (2016) Multifaceted thermoresponsive poly(N-vinylcaprolactam) coupled with carbon dots for biomedical applications. Mat Sci Eng C-Mater 61:492–498

101 Zhang L, Peng D, Liang RP, Qiu JD (2015) Nitrogen-doped graphene quantum dots as a new catalyst accelerating the coordination reaction between cadmium(II) and 5,10,15,20-tetrakis(1-methyl-4-pyridinio) porphyrin for cadmium(II) sensing. Anal Chem 87(21):10894–10901

102 Schlichting I, Miao J (2012) Emerging opportunities in structural biology with X-ray free-electron lasers. Curr Opin Struct Biol 22(5):613–626

103 Wu ZL, Gao MX, Wang TT, Wan XY, Zheng LL, Huang CZ (2014) A general quantitative pH sensor developed with dicyandiamide N-doped high quantum yield graphene quantum dots. Nanoscale 6(7):3868–3874

104 Gokhale R, Singh P (2014) Blue luminescent graphene quantum dots by photochemical stitching of small aromatic molecules: fluorescent nanoprobes in cellular imaging. Part Part Syst Charact 31(4):433–438

105 Guo RH, Zhou SX, Li YC, Li XH, Fan LZ, Voelcker NH (2015) Rhodamine-functionalized graphene quantum dots for detection of Fe^{3+} in cancer stem cells. ACS Appl Mater Interfaces 7(43):23958–23966

106 Zhang CF, Cui YY, Song L, Liu XF, Hu ZB (2016) Microwave assisted one-pot synthesis of graphene quantum dots as highly sensitive fluorescent probes for detection of iron ions and pH value. Talanta 150(1):54–60

107 Qian ZS, Ma JJ, Shan XY, Feng H, Shao LX, Chen JR (2014) Highly luminescent N-doped carbon quantum dots as an effective multifunctional fluorescence sensing platform. Chem Eur J 20(8):2254–2263

108 Campos BB, Abellan C, Zougagh M, Jimenez-Jimenez J, Rodriguez-Castellon E, Esteves da Silva JCG, Rios A, Algarra M (2015) Fluorescent chemosensor for pyridine based on N-doped carbon dots. J Colloid Interface Sci 458:209–216

109 Zuo PL, Xiao DL, Gao MM, Peng J, Pan RF, Xia Y, He H (2014) Single-step preparation of fluorescent carbon nanoparticles, and their application as a fluorometric probe for quercetin. Microchim Acta 181(11):1309–1316

110 Mao Y, Bao Y, Han DX, Li FH, Niu L (2012) Efficient one-pot synthesis of molecularly imprinted silica nanospheres embedded carbon dots for fluorescent dopamine optosensing. Biosens Bioelectron 38(1):55–60

111 Crist BV (1999) Handbook of the elements and native oxides. XPS International Inc, Mountain View

112 Li LB, Li L, Wang C, Liu KY, Zhu RH, Qiang H, Lin YQ (2015) Synthesis of nitrogen-doped and amino acid-functionalized graphene quantum dots from glycine, and their application to the fluorometric determination of ferric ion. Microchim Acta 182(3):763–770

113 Guo Y, Yang LL, Li WW, Wang XF, Shang YH, Li BX (2016) Carbon dots doped with nitrogen and sulfur and loaded with copper(II) as a "turn-on" fluorescent probe for cystein, glutathione and homocysteine. Microchim Acta 183(4):1409–1416

114 Li H, Shao FQ, Zou SY, Yang QJ, Huang H, Feng JJ, Wang AJ (2016) Microwave-assisted synthesis of N,P-doped carbon dots for fluorescent cell imaging. Microchim Acta 183(2):821–826

115 Nie H, Li MJ, Li QS, Liang SJ, Tan YY, Sheng L, Shi W, Zhang SXA (2014) Carbon dots with continuously tunable full-color emission and their application in ratiometric pH sensing. Chem Mater 26(10):3104–3112

116 Wang L, Zhou HS (2014) Green synthesis of luminescent nitrogen-doped carbon dots from milk and its imaging application. Anal Chem 86(18):8902–8905

117 Bhunia SK, Saha A, Maity AR, Ray SC, Jana NR (2013) Carbon nanoparticle-based fluorescent bioimaging probes. Sci Rep 3:1473

118 Ke CC, Yang YC, Tseng WL (2016) Synthesis of blue-, green-, yellow-, and red-emitting graphene-quantum-dot-based nanomaterials with excitation-independent emission. Part Part Syst Charact 33(3):132–139

119 Qian ZS, Ma JJ, Shan XY, Shao LX, Zhou J, Chen JR, Feng H (2013) Surface functionalization of graphene quantum dots with small organic molecules from photoluminescence modulation to bioimaging applications: an experimental and theoretical investigation. RSC Adv 3(34):14571–14579

120 Liu JJ, Zhang XL, Cong ZX, Chen ZT, Yang HH, Chen GN (2013) Glutathione-functionalized graphene quantum dots as selective fluorescent probes for phosphate-containing metabolites. Nanoscale 5(5):1810–1815

121 Liu MP, Liu T, Li Y, Xu H, Zheng BZ, Wang DM, Du J, Xiao D (2015) A FRET chemsensor based on graphene quantum dots for detecting and intracellular imaging of Hg^{2+}. Talanta 143:442–449

122 Zhou B, Shi BY, Jin DY, Liu XG (2015) Controlling anocrystals for emerging applications. Nat Nanotechnol 10:924–936

123 Cui YY, Hu ZB, Zhang CF, Liu XF (2014) Simultaneously enhancing up-conversion fluorescence and red-shifting down-conversion luminescence of carbon dots by a simple hydrothermal process. J Mater Chem B 2(40):6947–6952

124 Zhang YQ, Ma DK, Zhuang Y, Zhang X, Chen W, Hong LL, Yan QX, Yu K, Huang SM (2012) One-pot synthesis of N-doped carbon dots with tunable luminescence properties. J Mater Chem 22(33):16714–16718

125 Pan DY, Zhang JC, Li Z, Wu MH (2010) Hydrothermal route for cutting graphene sheets into blue-luminescent graphene quantum dots. Adv Mater 22(6):734–738

126 Zhu SJ, Zhang JH, Tang SJ, Qiao CY, Wang L, Wang HY, Liu X, Li B, Li YF, Yu WL, Wang XF, Sun HC, Yang B (2012) Surface chemistry routes to modulate the photoluminescence of graphene quantum dots: from fluorescence mechanism to up-conversion bioimaging applications. Adv Funct Mater 22(22):4732–4740

127 Kumar VB, Sheinberger Y, Porat Z, Shav-Tal Y, Gedanken A (2016) A hydrothermal reaction of an aqueous solution of BSA yields highly fluorescent N doped C-dots used for imaging of live mammalian cells. J Mater Chem B 4(17):2913–2920

128 Huang H, Lv JJ, Zhou DL, Bao N, Xu Y, Wang AJ, Feng JJ (2013) One-pot green synthesis of nitrogen-doped carbon nanoparticles as fluorescent probes for mercury ions. RSC Adv 3(44):21691–21696

129 Huang H, Xu Y, Tang CJ, Chen JR, Wang AJ, Feng JJ (2014) Facile and green synthesis of photoluminescent carbon nanoparticles for cellular imaging. New J Chem 38(2):784–789

130 Zheng XT, Than A, Ananthanaraya A, Kim DH, Chen P (2013) Graphene quantum dots as universal fluorophores and their use in revealing regulated trafficking of insulin receptors in adipocytes. ACS Nano 7(7):6278–6286

131 Yang ST, Cao L, Luo PG, Lu FS, Wang X, Wang HF, Meziani MJ, Liu YF, Qi G, Sun YP (2009) Carbon dots for optical imaging in vivo. J Am Chem Soc 131(32):11308–11309

132 Huang X, Zhang F, Zhu L, Choi KY, Guo N, Guo J, Tackett KN, Anilkumar P, Liu G, Quan Q, Choi HS, Niu G, Sun YP, Lee S, Chen X (2013) Effect of injection routes on the biodistribution, clearance, and tumor uptake of carbon dots. ACS Nano 7(7):5684–5693

133 Li Z, He XY, Wang Z, Yang RH, Shi W, Ma HM (2015) In vivo imaging and detection of nitroreductase in zebrafish by a new near-infrared fluorescence off–on probe. Biosens Bioelectron 63:112–116

134 Zhang YY, Shi W, Feng D, Ma HM, Liang Y, Zuo JR (2011) Application of rhodamine B thiolactone to fluorescence imaging of Hg^{2+} in *Arabidopsis thaliana*. Sensor Actuat B-Chem 153(1):261–265

135 Li LH, Li Z, Shi W, Li XH, Ma HM (2014) Sensitive and selective near-infrared fluorescent off − on probe and its application to imaging different levels of β-lactamase in *Staphylococcus aureus*. Anal Chem 86(12):6115–6120

136 Li Z, Gao XH, Shi W, Li XH, Ma HM (2013) 7-((5-Nitrothiophen-2-yl)methoxy)-3H-phenoxazin-3-one as a spectroscopic off-on probe for highly sensitive and selective detection of nitroreductase. Chem Commun 49(52):5859–5861

137 Guo LE, Zhang JF, Liu XY, Zhang LM, Zhang HL, Chen JH, Xie XG, Zhou Y, Luo K, Yoon J (2015) Phosphate ion targeted colorimetric and fluorescent probe and its use to monitor endogeneous phosphate ion in a hemichannel-closed cell. Anal Chem 87(2):1196–1201

138 Saxena M, Sonkar SK, Sarkar S (2013) Water soluble nano carbons arrest the growth of mosquito. RSC Adv 3(44):22504–22508

139 Zhai YL, Zhu ZJ, Zhu CZ, Ren JT, Wang EK, Dong SJ (2014) Multifunctional water-soluble luminescent carbon dots for imaging and Hg^{2+} sensing. J Mater Chem B 2(40):6995–6999

140 Ju J, Zhang RZ, He SJ, Chen W (2014) Nitrogen-doped graphene quantum dots-based fluorescent probe for the sensitive turn-on detection of glutathione and its cellular imaging. RSC Adv 4(94):52583–52589

141 Zhang M, Bai LL, Shang WH, Xie WJ, Ma H, Fu YY, Fang DC, Sun H, Fan LZ, Han M, Liu CM, Yang SH (2012) Facile synthesis of water-soluble, highly fluorescent graphene quantum dots as a robust biological label for stem cells. J Mater Chem 22(15):7461–7467